1987

Processing and superplasticity in lithium-containing Al-Mg alloys.

Sanchez, Benjamin W.

NAVAL POSTGRADUATE SCHOOL
Monterey, California

THESIS

PROCESSING AND SUPERPLASTICITY IN
LITHIUM-CONTAINING Al-Mg ALLOYS

by

Benjamin W. Sanchez

March 1987

Thesis Advisor: T. R. McNelley

Approved for public release; distribution is unlimited

REPORT DOCUMENTATION PAGE

UNCLASSIFIED

1a REPORT SECURITY CLASSIFICATION	1b RESTRICTIVE MARKINGS
2a SECURITY CLASSIFICATION AUTHORITY	3 DISTRIBUTION/AVAILABILITY OF REPORT: Approved for public release; distribution is unlimited.
2b DECLASSIFICATION/DOWNGRADING SCHEDULE	
4 PERFORMING ORGANIZATION REPORT NUMBER(S)	5 MONITORING ORGANIZATION REPORT NUMBER(S)
6a NAME OF PERFORMING ORGANIZATION: Naval Postgraduate School / 6b OFFICE SYMBOL (If applicable): Code 69	7a NAME OF MONITORING ORGANIZATION: Naval Postgraduate School
6c ADDRESS (City, State, and ZIP Code): Monterey, California 93943-5000	7b ADDRESS (City, State, and ZIP Code): Monterey, California 93943-5000
8a NAME OF FUNDING/SPONSORING ORGANIZATION / 8b OFFICE SYMBOL (If applicable)	9 PROCUREMENT INSTRUMENT IDENTIFICATION NUMBER
8c ADDRESS (City, State, and ZIP Code)	10 SOURCE OF FUNDING NUMBERS: PROGRAM ELEMENT NO / PROJECT NO / TASK NO / WORK UNIT ACCESSION NO

11 TITLE (Include Security Classification)

PROCESSING AND SUPERPLASTICITY IN LITHIUM-CONTAINING Al-Mg ALLOYS.

12 PERSONAL AUTHOR(S)
SANCHEZ, BENJAMIN W.

13a TYPE OF REPORT	13b TIME COVERED	14 DATE OF REPORT (Year, Month, Day)	15 PAGE COUNT
Master's Thesis	FROM _____ TO _____	1987 March	53

16 SUPPLEMENTARY NOTATION

17 COSATI CODES			18 SUBJECT TERMS (Continue on reverse if necessary and identify by block number)
FIELD	GROUP	SUB-GROUP	Al-Mg-Li, Superplasticity, Superplastic Deformation, Thermomechanical Processing

19 ABSTRACT (Continue on reverse if necessary and identify by block number)

The refined microstructures and superplastic properties resulting from controlled thermomechanical processing of a Al-8Mg-0.5Li-0.2Zr alloy were evaluated. The processing involved warm rolling at 300°C separately to true strains of 1.9 and 2.6. Increasing the rolling strain enhanced the superplastic ductility of the alloy at 300°C in the strain rate regime of 10^{-2}-$10^{-3}S^{-1}$. Elongations in excess of 500 pct., without cavitation, and a corresponding strain rate sensitivity coefficient of approximately 0.5, were obtained. TEM investigations of the microstructural characteristics responsible for the mechanical behavior revealed that a more uniformely refined grain structure (2-5μm) evolved by continuous recrystallization in material experiencing the larger rolling strain. It was also concluded that the increase in rolling strain enhances grain refinement both preceding and concurrent with superplastic deformation.

20 DISTRIBUTION/AVAILABILITY OF ABSTRACT	21 ABSTRACT SECURITY CLASSIFICATION
☒ UNCLASSIFIED/UNLIMITED ☐ SAME AS RPT ☐ DTIC USERS	Unclassified
22a NAME OF RESPONSIBLE INDIVIDUAL: Terry McNelley	22b TELEPHONE (Include Area Code): (408)646-2589 / 22c OFFICE SYMBOL: 69Mc

DD FORM 1473, 84 MAR — 83 APR edition may be used until exhausted. All other editions are obsolete.

Approved for public release; distribution is unlimited.

Processing and Superplasticity in Lithium-Containing Al-Mg Alloys

by

Benjamin W. Sanchez
Lieutenant, United States Navy
B.E., SUNY Maritime, 1979

Submitted in partial fullfillment of requirements for the degree of

MASTER OF SCIENCE IN MECHANICAL ENGINEERING

from the

NAVAL POSTGRADUATE SCHOOL
March 1987

ABSTRACT

The refined microstructures and superplastic properties resulting from controlled thermomechanical processing of a Al-8Mg-0.5Li-0.2Zr alloy were evaluated. The processing involved warm rolling at 300°C separately to true strains of 1.9 and 2.6. Increasing the rolling strain enhanced the superplastic ductility of the alloy at 300°C in the strain rate regime of 10^{-2}-$10^{-3}s^{-1}$. Elongations in excess of 500 pct., without cavitation, and a corresponding strain rate sensitivity coefficient of approximately 0.5, were obtained. TEM investigations of the microstructural characteristics responsible for the mechanical behavior revealed that a more uniformely refined grain structure (2-5μm) evolved by continuous recrystallization in material experiencing the larger rolling strain. It was also concluded that the increase in rolling strain enhances grain refinement both preceding and concurrent with superplastic deformation.

TABLE OF CONTENTS

LIST OF FIGURES

ACKNOWLEDGEMENT

I would like to thank my advisor, Professor T. R. McNelley for his professional guidance, and Dr. S. J. Hales for his expert work in the TEM microscopy needed for this work. Additionally, I would like to thank LT James Wise, LT Don Stewart and CDR Dimos Solomos, whose current thesis research provided a helping hand when needed.

I. INTRODUCTION

Superplasticity today is no longer the unusual phenomena reported on by Underwood in a review paper in 1962 [Ref. 1], but a well established and growing part of today's metallurgical practice. A simple definition of superplastic behavior is the ability of a material to sustain large tensile elongations as a result of resistance to necking. The interest in such behavior is not only for scientific but for practical and economic reasons as well. Industry's desire to fabricate structures of greater strength without increasing weight and by less time- and energy-consuming processes is a worthwhile goal both mechanically and financially.

An interesting example of the benefits of superplasticity is a time-cost analysis for a generic aircraft nose door assembly [Ref. 2: p. 403]. Tooling and assembly hours for conventional fabrication, (fasteners and rivets), add up to over 3700 hours. With superplastic forming techniques the total drops to 500 hours.

Research at the Naval Postgraduate School (NPS) has centered on high-Mg, Al-Mg-X alloys. The superplastic results achieved with these alloys have come about as a result of thermomechanical processing (TMP) experimentation. In addition to the TMP, variations in alloy additions are a part of this research. The specific alloy addition of interest here is Lithium.

Previous work by Oster [Ref. 3], delt with the effects of the TMP on two Al-Mg-X alloys with 0.5% and 1.0% weight percent of Lithium. This thesis is a continuation of Oster's work. The intention here is to

increase rolling strain during the TMP on the Al-8.0%Mg-0.5Li-0.23%Zr alloy, (NPGS 1), study the mechanical and microstructural effects and thereby develop a greater understanding of Superplastic Deformation (SPD) mechanisms.

II. BACKGROUND

As the use of SPD in manufacturing increases, there is a growing need to understand the mechanisms involved. The effect of alloy additions, of thermomechanical processing and the forming techniques must be studies so that present systems can be improved upon and new materials developed. Many alloys have been seen to exhibit superplastic behavior. The choice of the material usually depends on its intended use, as well as its cost and availability. The aircraft and aerospace industries depend on light-weight, strong alloys and this research is funded by the U.S. Naval Air Systems Command.

A. Al-8.0%Mg-0.5%Li-0.23%Zr

Aluminum is a light weight, strong and corrosion resistant metal that has been the basis for many aircraft alloys for decades. All the advantages of Aluminum need not be repeated here. The additions in this alloy, though, do require more attention.

Magnesium is a common alloying element with Aluminum. It is the major addition in the 5XXX series Aluminum alloys and is also present in the 6XXX and 7XXX series. The weight-percent Mg in NPGS 1 is higher than normally found in Al alloys and this fact is important to the superplastic behavior.

During the warm working stage of the TMP, β, a second phase, is precipitated, [Ref. 4: p. 1043]. This β is identified as Al_8Mg_5 by Mondolfo [Ref. 5: pp. 312-313] and as Al_3Mg_2 by Massalski [Ref. 6: pp. 129-130]. Mondolfo's composition for the β is the one accepted in this work. The effect of the β on the subgrain/grain structure is the primary

consideration here. A fine and uniformly distributed β, or any second phase, may exert a stabalizing effect on the microstructure by retarding dislocation and boundary motion. In addition to stabilizing subgrain/grain structures, it also can act to retard grain coarsening during SPD. With this high Mg content, a large percentage of Al_8Mg_5 may be expected to precipitate under appropriate conditions and thereby affect the matrix according to its size and distribution.

The Zirconium plays an important role in the alloy. In the form Al_3Zr this metastable phase acts as a subgrain/grain refiner during recrystallization. Al_3Zr precipitates as a very small particles. These small particles are effective in pinning grain boundaries and slowing down grain growth, [Ref. 7].

Lithium is the lightest of all the metals and, compared to Aluminum, is only 20 percent as dense. In this alloy the Lithium is not used to enhance superplasticity. Its addition is meant to reduce the overall density and at the same time increase the elastic modulus. For every one percent of Lithium used, the density of an alloy is expected to decrease by three percent due to its replacing heavier elements [Ref. 8:pp. 57]. The strengthening effect attributed to Lithium arises from the formation of metastable second phase, Al_3Li. According to the phase diagram proposed by Sigili and Sanchez, Figure 2.1, [Ref. 9] with a 0.5 weight percent Lithium (1.9 atomic percent) Al_3Li precipitates at ~423K (150°C). This is well below the superplastic forming temperature of 573K (300°C) used in this work and described later in this thesis. At the superplastic forming temperature the Lithium is therefore in solution and would not be expected to effect SPD except as a solute. As the alloy cools after

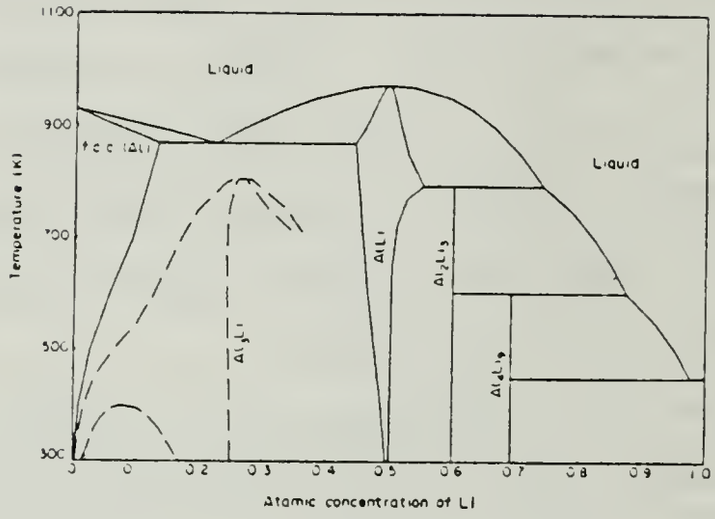

Figure 2.1. Al-Li Phase Diagram

deformation the Al_3Li phase precipitates. It then forms very small, spherical particles throughout the matrix providing a precipitation strenthening effect at ambient temperature.

B. SUPERPLASTICITY

Theories for superplastic behavior differ and no one model encompasses all the possible influences associated with SPD. A phenomenological relation for superplastic deformation that has growing acceptance is one by Sherby and Wadsworth [Ref. 10]. The equation and terms are:

$$\dot{\varepsilon}_{spd} = A \frac{D^*_{eff}}{d^p} \left(\frac{\sigma}{E}\right)^n \qquad 2.1$$

$\dot{\varepsilon}_{spd}$ = strain rate during SPD

A = material constant

D^*_{eff} = effective diffusion coefficient

d = grain size

p = grain size exponent

σ = stress

E = Young's modulus

n = stress component = $\frac{1}{m}$

m = strain rate sensitivity coefficient

Before the significance of this equation is explained the values of the exponents n and p must be discussed. It is generally accepted that superplastic flow occurs when $n<2$ ($m>0.5$). The strain rate sensitivity coefficient m is determined from the slope of the stress versus strain-rate curve on log-log axis ($m=d\ln\sigma/d\ln\dot{\varepsilon}$). This relationship σ versus $\dot{\varepsilon}$, is most often sigmoidal in shape and is discussed in terms of three regions, Figure 2.2.

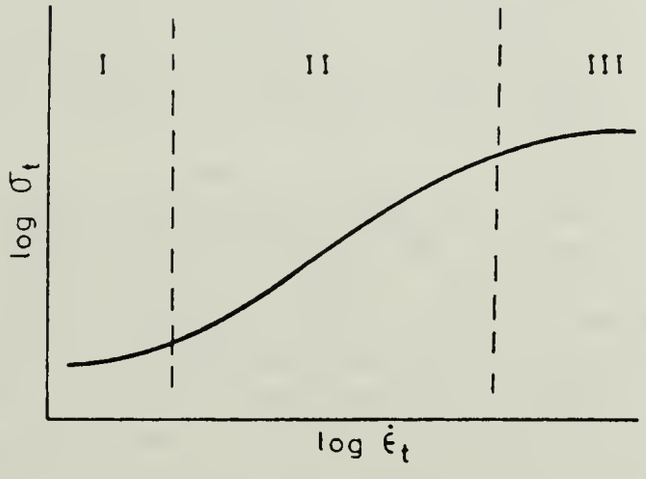

Figure 2.2. Stress Versus Strain Rate

Region I (low $\dot{\varepsilon}$) is thought to be associated with diffusion creep and threshold effects although the data for this region are sparse and open to disagreement. Region III (high $\dot{\varepsilon}$) is more widely accepted to be dominated by dislocation mechanisms. The segment between I and III is marked by an inflection point that corresponds to the steepest slope of this curve, i.e.; the larger m-value. This is region II where peak ductilities

are obtained. In region II, where $m \geq 0.5$ and superplastic flow occurs, Grain Boundary Sliding (GBS) is considered as the dominant deformation mechanism, [Ref. 10]. If GBS is the prevailing process then the associated grain size exponent p , equals 2.

Two of the terms in equation 2.1 should be singled out and examined. These terms are $\frac{1}{d^p}$ and σ^n. Rewritten with p and n equal to two leads to a model where:

$$\dot{\varepsilon}_{spd} \sim \left(\frac{\sigma^2}{d^2}\right) \qquad 2.2$$

This relationship indicates the effect of grain size on superplasticity and can be thought of as a balance. When the material is deformed at an elevated temperature and the grain size begins to coarsen, the flow stress must increase proportionally if the imposed strain rate is held constant. as long as the grain size remains stable the balance allows GBS to remain the dominant mechanism.

As noted in part A of this chapter the alloying elements in this material effect the grain size. Al_3Zr is a grain refiner during recrystallization and both the β and the Al_3Zr act to stabilize the microstructure and to retard grain growth. The degree to which these two phases contribute will be a key part of this work.

C. METHODS OF GRAIN REFINEMENT

To achieve a fine grain structure capable of sustaining SPD, thermomechanical processing is used. The mechanical working during the TMP introduces a very high dislocation density. The large amount of stored energy associated with this dislocation structure acts to provide a driving

force for recovery processes to rearrange the dislocations into a cellular arrangment where the dislocation density in cell interiors is much reduced, [Ref. 11:p. 12]. Recovery is generally not viewed as a recrystallization process as it does not alter the orientation of the crystal lattice. In the next step of the grain refinement, recrystallization occurs. From the recovered structure new grains form by either a discontinuous or continuous recrystallization mode.

Discontinuous recrystallization is a process of nucleation and growth by grain boundary migration that results in the formation of new, strain free grains. The size of these new grains may tend to be large if there is a lack of any retarding influences. Without control over this growth, the microstructure is unable to support superplastic behavior as indicated by the grain size component of equation 2.2.

Development by continuous recrystallization does not involve nucleation and growth by boundary migration but rather a gradual coalescence into a grain structure from the recovered state. These new grains develope boundary misorientations that are adequate to stabilize the grain size and resist further coarsening. The amount of misorientation necessary to result in a stabilize microstructure and allow for GBS is an ongoing question. Work by Hales and McNelley [Ref. 12] on a Al-Mg alloy with similar TMP showed that misorientation of less than 10° are sufficient. Although a misorientation study is beyond the scope of this thesis work, microstructural examination of the material after warm working and before and after SPD should be able to support a conclusion of which recrystallization process occured.

D. RESEARCH AT THE NAVAL POSTGRADUATE SCHOOL

Extensive work has been done at NPS on the Al-Mg alloys. The first work by McNelley and Garg [Ref. 13] considered methods of TMP to achieve the fine microstructure necessary for SPD. This ongoing research also includes effects of alloy additions as well as recrystallization models [Ref. 3, 4, 11-16].

Previous work by Oster [Ref. 3] initiated study of the Al-8%Mg-0.5%Li-0.23%Zr alloy. The TMP used in that work warm rolled the material to 85 percent reduction (a true strain of 1.9). The resulting elevated temperature testing of the material produced only moderate ductilities. Oster suspected that greater initial reduction during rolling might produce greater ductilities. The aim of this work is to increase the rolling reduction during TMP and observe its effects on microstructure, recrysallization processes and ductility. Explanation of these results in terms of our current understanding of superplastic behavior will then be attempted.

III. EXPERIMENTAL

A. MATERIAL PROCESSING

The alloy designated, NPGS 1, was cast into tapered cylindrical ingots by the Naval Surface Weapons Center, White Oak, Maryland. Composition varied slightly from surface to the center according to chemical analysis, [Ref. 17]; nominal composition by weight percent was Al-8%Mg-0.5%Li-0.23%Zr.

The thermomechanical processing method employed was developed at the Naval Postgraduate School. The cast ingot was cut into rectangular billets approximately 1.1" x 1.1" x 2.8". Each billet was then solution treated for 5 hours at 713K (440°C) followed by 19 hours at 753K (480°). The solution treatment at 713K is above the Mg solves ~608K (355°C) but below the eutectic 723K (450°C), [Ref. 18]. This is done to avoid melting of any nonequilibrium β (Al_8Mg_5) initially present. Final treatment at 753K ensures homogenization of any other second phases present. At the end of the twenty four hour solution treatment the billets were upset forged on plattens heated to 753K. Forging reduced the billets' height by approximately two thirds. After forging, the billets were replaced in the furnace at 753K for 1 hour, followed by a vigorous oil quench.

The final step in the TMP was warm working the material by isothermal rolling at 573K (300°C). To facilitate the rolling process the forged billets were trimmed. The billets were initially heated for 30 minutes at 573K prior to the first rolling pass. Between each pass the billets were returned to the furnace for 4 minutes to ensure isothermal working.

Two different rolling procedures, each involving a different reduction per pass, were employed: a 1mm per pass scheme and the other a 2.5mm per pass scheme. It was desired to achieve a total strain of 2.6 for each billet with the two different rolling reductions. The 1mm per pass billet achieved a total strain of 2.6 while the 2.5mm per pass billet only reached a 2.25 total strain. Upon completion of the final pass, the material was quenched in oil. Figure 3.1 graphically illustrates this TMP.

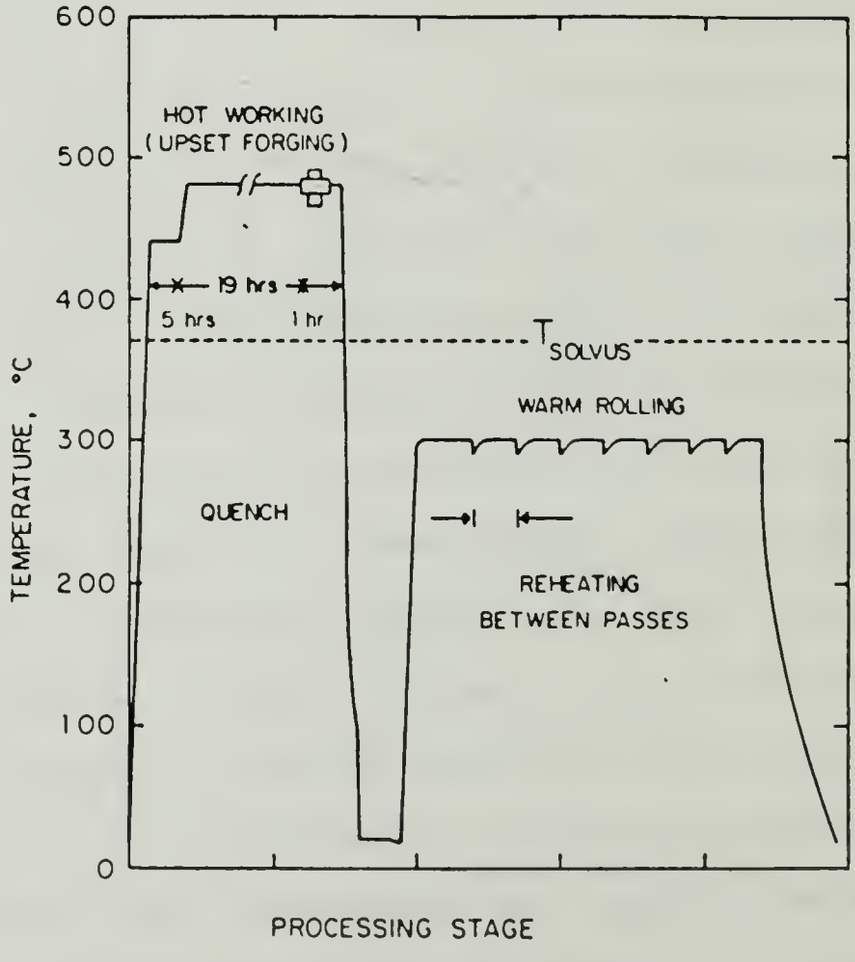

Figure 3.1. Schematic of the Thermomechanical Processing

Elevated temperature tensile specimens were cut from the rolled billets with tensile axis parallel to the rolling direction. The specimens

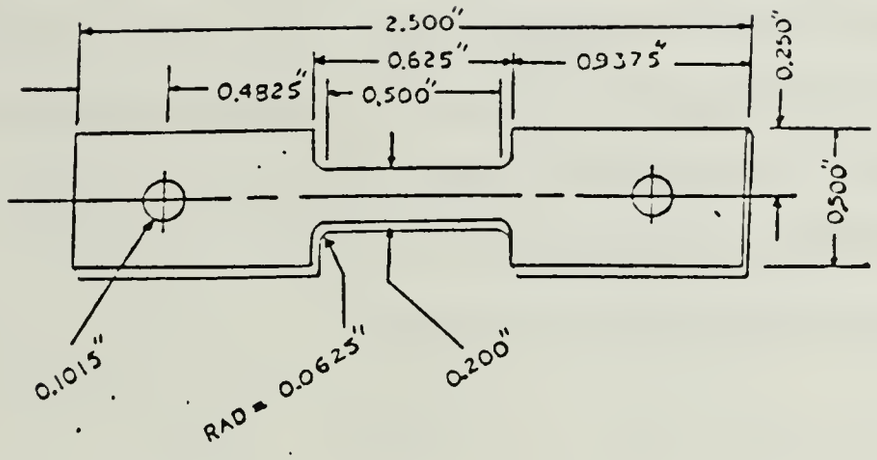

Figure 3.2. Tensile Specimens Geometry

geometry, Figure 3.2, was that used by Alcamo [Ref. 16]. Each piece was lightly marked 0.5" apart in the gage section for measurement after SPD. Cross sectional area was recorded for all the tensile specimens in the gage section.

B. SPECIMEN TESTING

The elevated temperature tests were performed on an Instron machine, model TT-D. The tensile specimens were held in a wedge and pin grip arrangement. A Marshall three zone model 2232 clam shell furnace was used to maintain a uniform temperature of 573K (300°C) during the test. The temperature took approximately 45 to 60 minutes to stabilize prior to each test. This was monitored by four internally mounted thermocouples.

Initial strain rates were varied from $6.67 \times 10^{-5} s^{-1}$ to $1.67 \times 10^{-1} s^{-1}$. Each test was done at a constant nominal strain rate. All samples were pulled to failure and load versus time data for each test was automatically plotted by the Instron machine.

C. DATA REDUCTION

The calculations and reduction of the load versus time data was done on an IBM XT computer using a "Basic" language program. Engineering stress and strain were computed, then used to calculate true stress and true strain. The equations used were:

Engineering stress $$S = \frac{F}{A_o}$$

Engineering strain $$e = \frac{L_f - L_o}{L_o}$$

True stress $$\sigma = S(1+e)$$

True strain $$\varepsilon = \ln(1+e)$$

where: F = load

A_o = original cross sectional area of tensile specimens

L_f = final length between gage section marks

L_o = original length between gage section marks.

The reduction of data using the equations listed above also include a scale factor to compensate for deformation outside of the grip section during each tensile test, [Ref. 19]. A separate scale factor is calculated for each load versus time curve. This compensation allows for the direct comparison of data at the various strain values.

D. TEM METALLOGRAPHY

Thin foil TEM samples were prepared using an electrolyte of 25% HNO_3 in methanol at 253K (-20°C) in a Struers electropolisher set at 15 vdc. Gage section specimens were taken as close to the fracture as possible.

Grip samples were from an area away from the grip pin hole and as-rolled material from the center of the rolled billet. Thin foils of material tested by Oster [Ref. 3] were also prepared for examination. Foil normals were always parallel to the sheet normal. The foils were examined in a JEOL-100CX II Transmission Electron microscope operated at 120KV. Each foil used was carefully placed in the sample holder to ensure the rolling direction was known during examination.

IV. RESULTS AND DISCUSSION

As noted earlier this current effort is intended to extend the work of Oster by altering the TMP. Two variables were changed from that previous work. First was an increase in the total strain during the warm rolling and the other was use of a larger strain per pass, i.e., a heavier rolling reduction rate. The results and discussion below are grouped according to these changes.

A. INCREASED TOTAL WARM ROLLING STRAIN

1. As Rolled Condition

The TMP procedures used by Oster, [Ref. 3] and in this work were nearly identical. The difference in the two processes lies in the extent of the warm working carried out. Oster ended the TMP at an 85% reduction (1.9 total warm rolling strain) while here, the reduction was extended to 93% (2.6 total warm rolling strain).

Microstructural comparison of the rolled condition of the two total warm rolling strains show little difference. Microscopy done by Oster, Figure 4.1, shows a very high dislocation density obscuring all other details. A similar microstructure is evident with 2.6 total strain, Figure 4.2. In darkfield, Figure 4.1(b), the β that is visible appears to be larger and coarser with the lesser rolling strain compared to the β visible in darkfield Figure 4.2(b). Observation of the β in either case was made difficult because of the high dislocation density.

2. Microstructure at the Onset of SPD

Before tensile specimens fabricated from as rolled material are tested, they undergo 45 to 60 minutes of heating at a temperature of 573K (300°C). This is the time it takes the furnace temperature to stabilize.

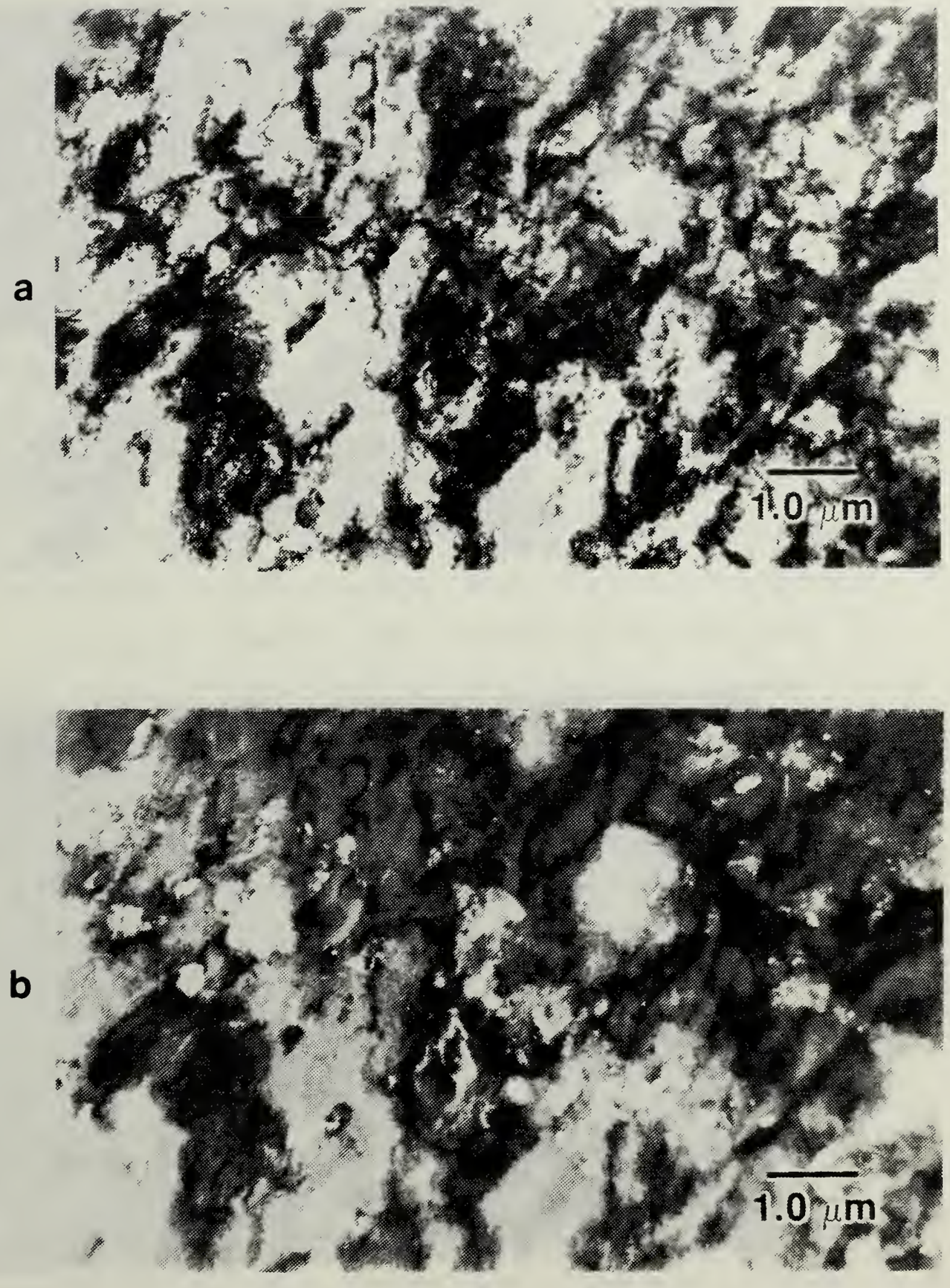

Figure 4.1. A Bright field (a), Dark field (b) Pair of TEM Micrographs of the As-Rolled Condition. Material Preparation and Microscopy Done by Oster, [Ref. 3], at a Total Warm Rolling Strain of 1.9.

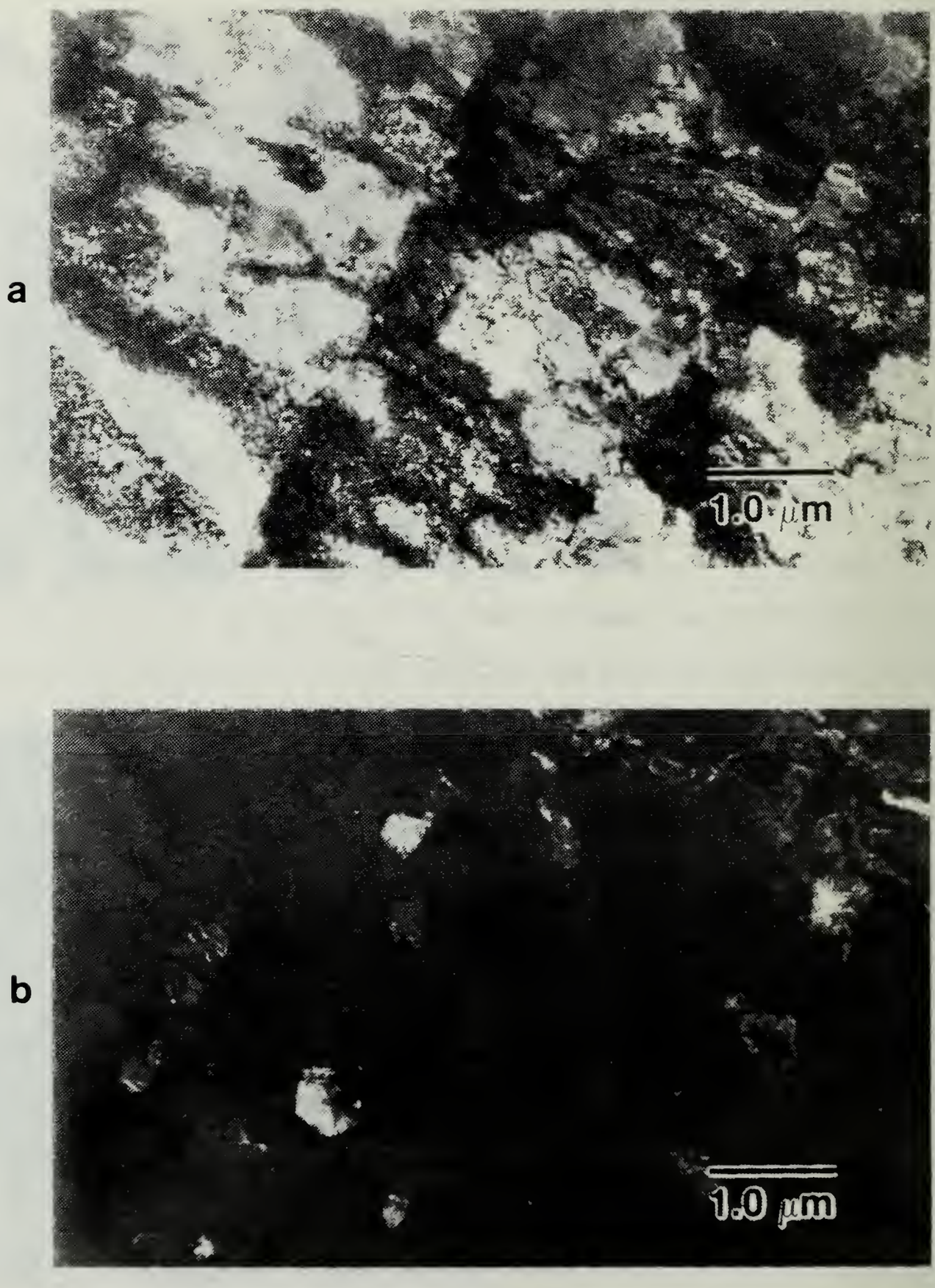

Figure 4.2. A Bright field (a), Dark field (b) Pair of TEM Micrographs of the As-Rolled Condition, at the Greater Total Warm Rolling Strain of 2.6 Utilized in This Work.

To examine the microstructural changes associated with this heating, samples were taken from grip sections of tensile specimens tested at a strain rate of $1.67 \times 10^{-1} S^{-1}$. At this strain rate, failure occurs in less than 15 seconds and thus the structure of the grip section should be representative of the microstructure at the onset of the elevated temperature deformation process for any of the strain rates employed. Grip sections of test samples remaining from Oster's work were prepared for TEM examination as well as grip sections from samples of this work. Figure 4.3 illustrates the microstructural changes resulting from the increase of the total warm rolling strain from 1.9 to 2.6. It is quite evident that the larger total strain resulted in a finer, more equiaxed grain structure.

As previously suggested in the comparison of the as-rolled structures, Figure 4.4 and 4.5 clearly show a fine, more uniformly distributed β in material experiencing the larger total warm rolling strain. The continued rolling appears to break up the β . A stringer of β particles is seen in Figure 4.4 and such structures were prevalent throughout the TEM examination of grip sections from Oster's samples. Very few of these β stringers could be found in the grip sections of samples experiencing the 2.6 total strain.

The development of this fine microstructure, especially for the larger warm rolling strain, is consistent with mechanisms of continuous recrystallization [Ref. 12,20]. Both materials recover from the high dislocation density produced by the rolling and undergo coalesence into a fine structure, but the larger 2.6 total warm rolling strain produces the finer grain size likely due to a greater initial dislocation density.

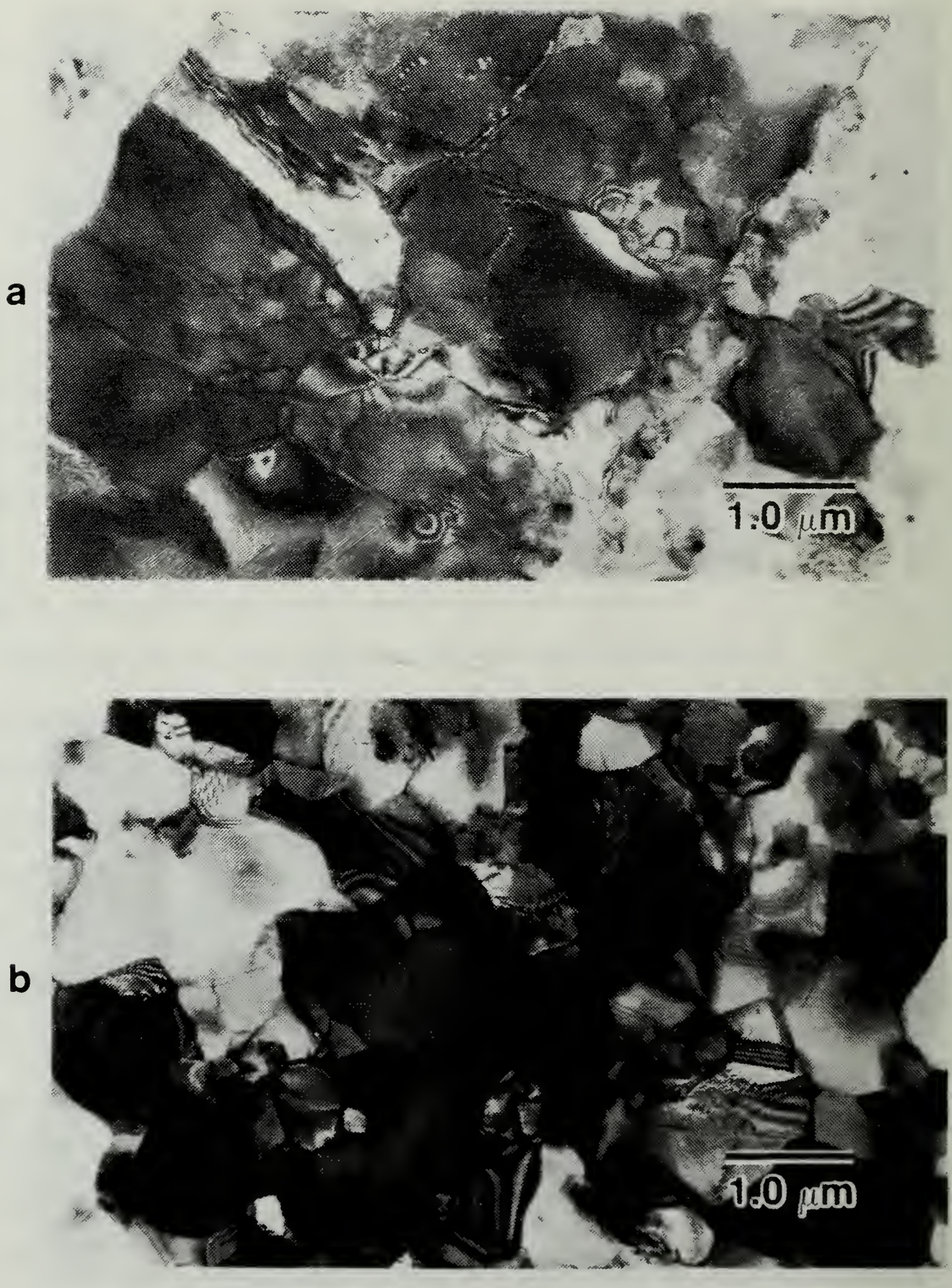

Figure 4.3. TEM Micrographs of Tensile Specimen Grip Sections Having a Total Warm Rolling Strain of 1.9(a) and 2.6(b), Respectively. Samples in both cases have experienced approximately 45 to 60 minutes at temperatures subsequent to the rolling.

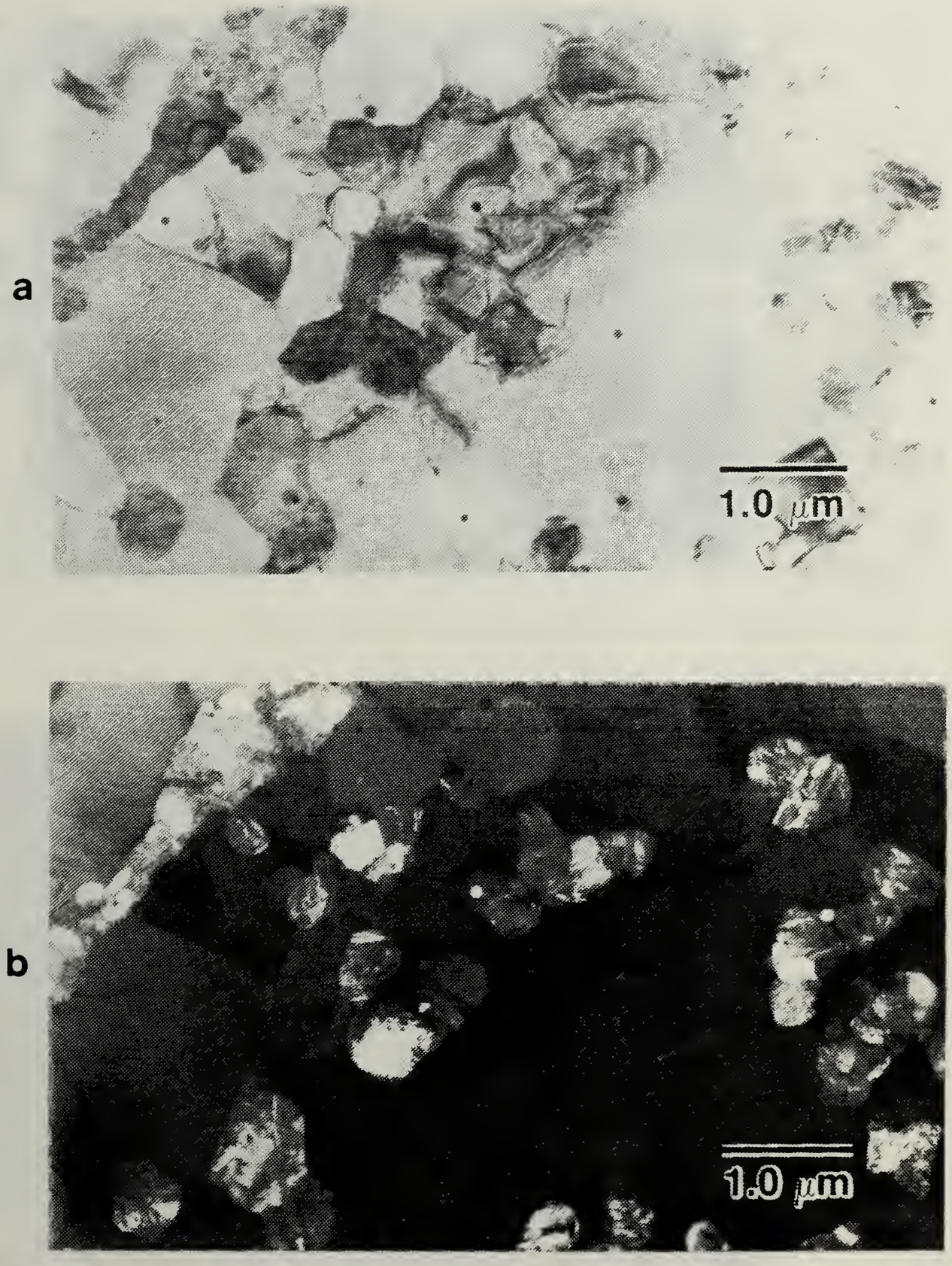

Figure 4.4. A Bright field (a), Dark field (b) Pair of TEM Micrographs Illustrating the Distribution of β in the Grip Section of Samples Experiencing 1.9 Total Warm Rolling Strain. Micrographs were obtained from the grip section of a sample experiencing approximately 45 to 60 minutes at temperature.

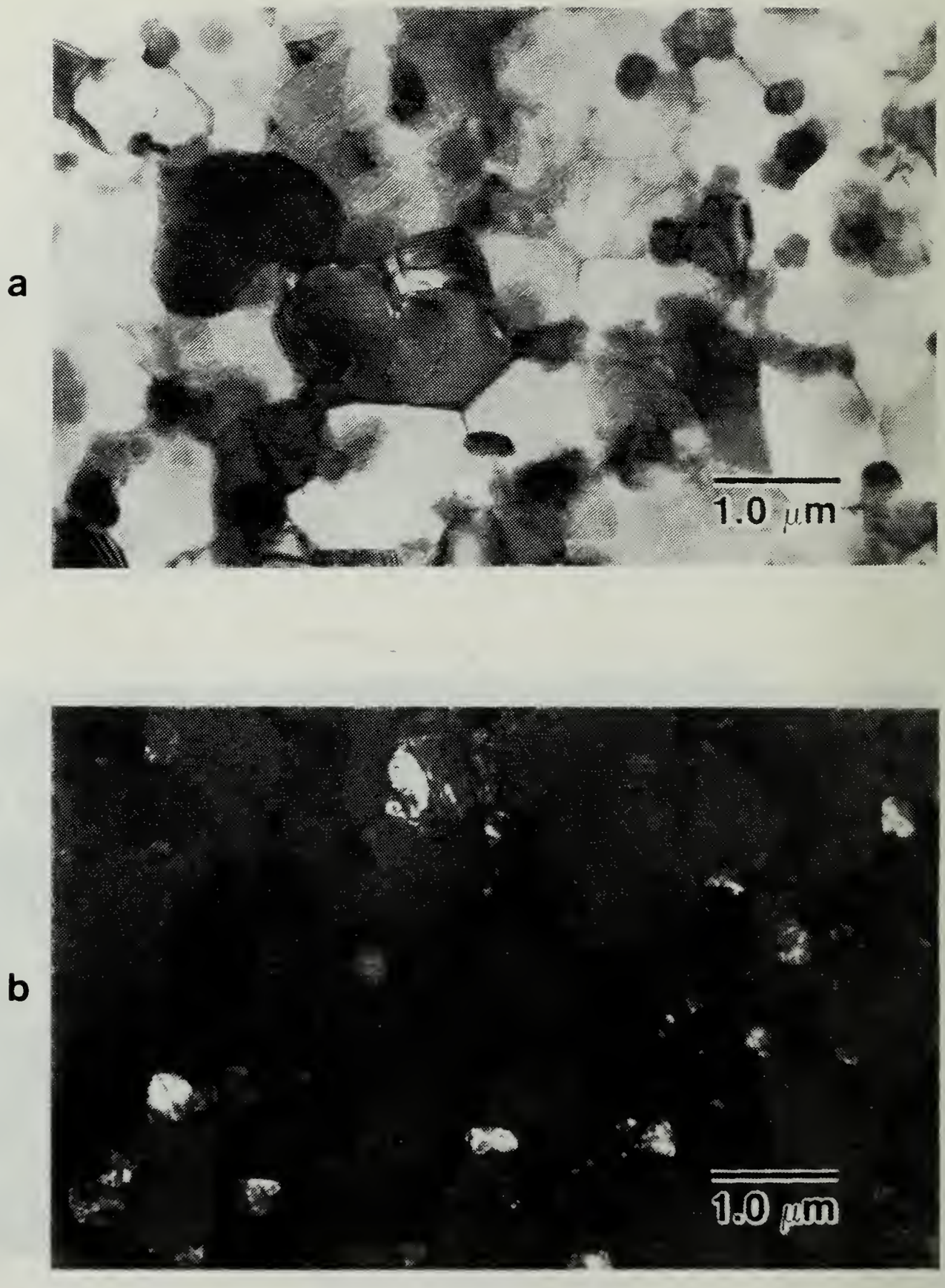

Figure 4.5. Representative β Distribution Illustrated by the Bright field (a), Dark field (b), Pair of TEM Micrographs From the Grip Section of Samples Experiencing the 2.6 Total Warm Rolling Strain and Approximately 45 to 60 Minutes at Temperature.

As discussed by Hales and McNelley [Ref. 12] this increase in warm rolling strain may result in the development of misorientations large enough, during the recovery recrystallization stage, to give a stable boundary structure. If the misorientations are large enough, then such boundaries would be able to accomodate GBS. With a fine grain size and adequate misorientations to stabilize the structure and allow for GBS the material would be expected to behave superplastically.

Further comparisons of these grip sections suggest that the Al_3Zr acts as a grain refiner equally for both materials. The observation of a finer β in the material experiencing the greater rolling reduction indicates that the β may also assist in stabilizing the final grain size and therefore produce a finer result. The coarser β particles in Oster's material are too large to act as effectivly in stabilizing the grain size. Additionally, scanning the entire thin foil area of Oster's grip section sample showed regions devoid of any β . These areas would lack any of the advantages β may provide.

3. Elevated Temperature Tests

The elevated temperature test data in the form of true stress versus true strain, is shown in Figure 4.6 for the material processed in this work. These data are then used to plot the flow stress versus strain rate and thereby obtain the strain rate sensitivity coefficient, i.e., the m value.

Figure 4.7 is a comparison of the flow stress versus strain rate data for Oster's data on material experiencing 1.9 total strain and the material of this effort with 2.6 total warm rolling strain. All graphical data concerning the 1.9 total strain material was previously reported by

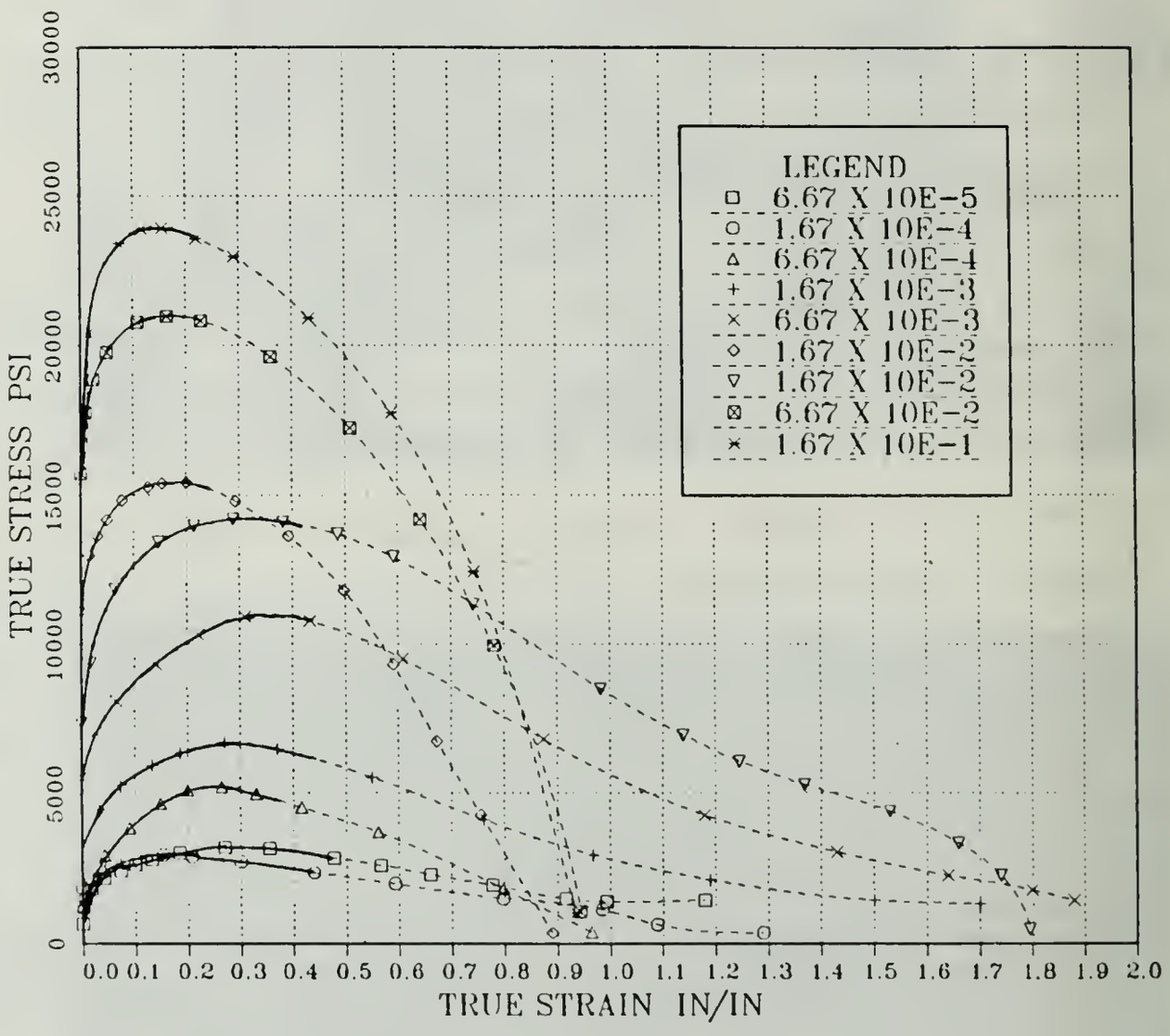

Figure 4.6. True Stress Versus True Strain at 573°K (300°C) for Superplastically Deformed Tensile Specimens. The 1mm reduction per pass during warm rolling, resulted in a total strain of 2.6. Strain rates were varied from $10^{-5}S^{-1}$ to $10^{-1}S^{-1}$ as indicated.

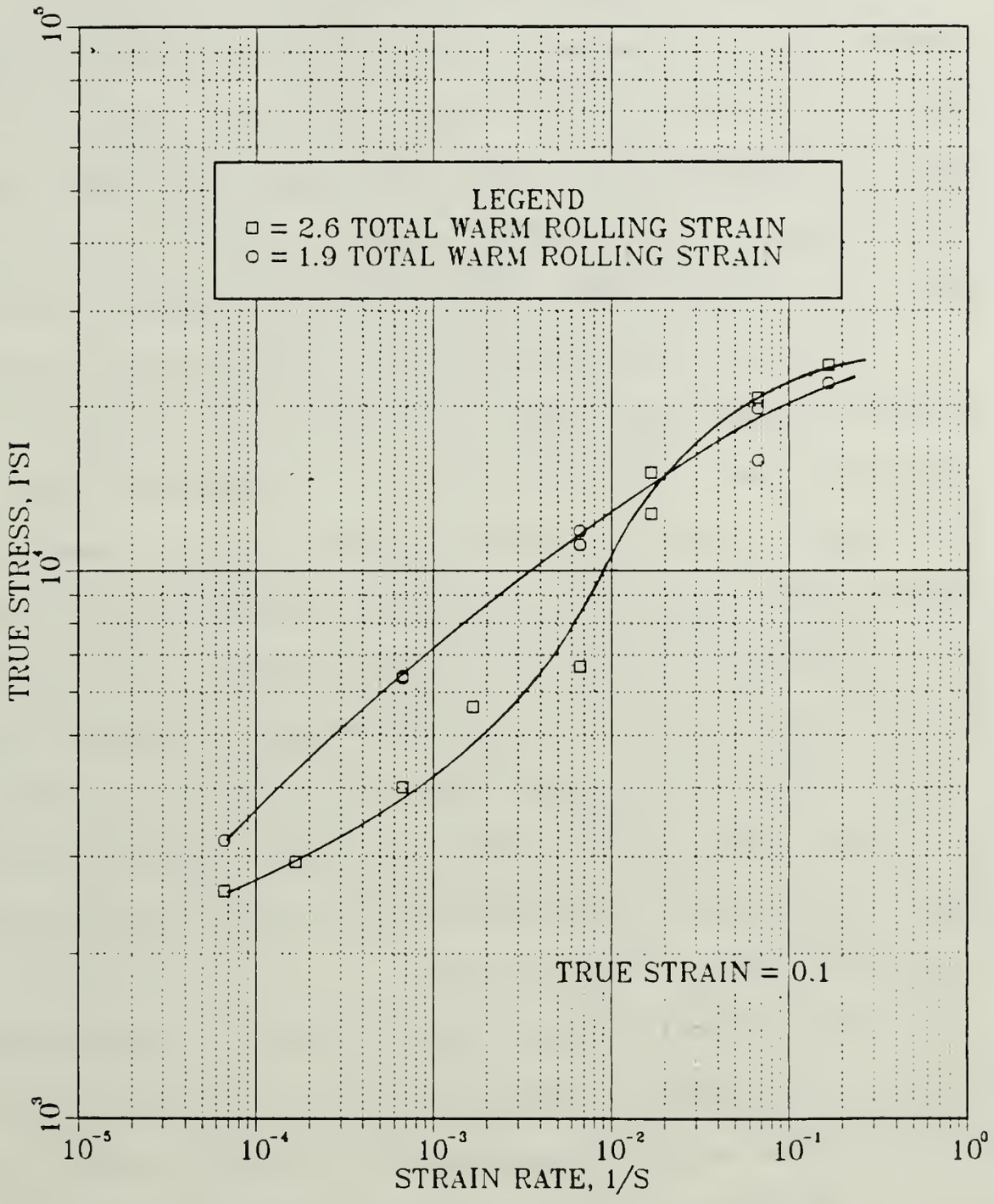

Figure 4.7. True Stress Versus Strain Rate Data for a True Strain of 0.1. The increase in total warm rolling strain caused a decrease in flow stress. This also resulted in an increase in the maximum strain rate sensitivity coefficient from 0.31, [Ref. 3] to ≈0.5.

Oster [Ref. 3] and is included here for direct comparison of the effect of increased rolling reduction.

Two important observations can be made from Figure 4.7. First, the flow stress decreases as result of the increase in rolling strain. Second, the m-value increases for the larger total strain. Oster's maximum m-value was 0.31 compared to 0.5 for this work. These observations suggest that at the test temperature 573K (300°C), the larger total strain produces a some what softer material, which in turn could lead to greater ductility.

The m-value associated with grain boundary sliding, as the dominant mechanism in superplastic flow, is 0.5 [Ref. 10]. Without yet looking to the ductility data and microstructure, it is evident that most all the requirements necessary to produce superplastic behavior have been achieved. Ductility data, Figure 4.8, clearly shows the effect of the increased total warm rolling strain. The 1.9 total strain produced a peak ductility of 293% at $\dot{\varepsilon} = 6.67 \times 10^{-4} S^{-1}$. A maximum ductility of 556% was obtained at $\dot{\varepsilon} = 6.67 \times 10^{-3} S^{-1}$ for the greater warm rolling strain. The 556% peak occurs in the same strain rate range where the maximum m-value of 0.5 occurs, Figure 4.7. Also, peak ductilities occured in this work at higher strain rates, $10^{-3} S^{-1}$ vice $10^{-4} S^{-1}$ for Oster.

TEM micrographs, Figures 4.9, 4.10 and 4.11, are comparison of the microstructure present in gage section at the two different total warm rolling strains, and at a $\dot{\varepsilon} = 6.67 \times 10^{-3} S^{-1}$ where this effort's greatest ductility was observed. As with the grip sections, gage samples from Oster were also prepared for this microstructural comparison. Overall, the greater total warm rolling strain material, Figure 4.9 has a slightly smaller grain size and fewer dislocations after SPD. The differences are

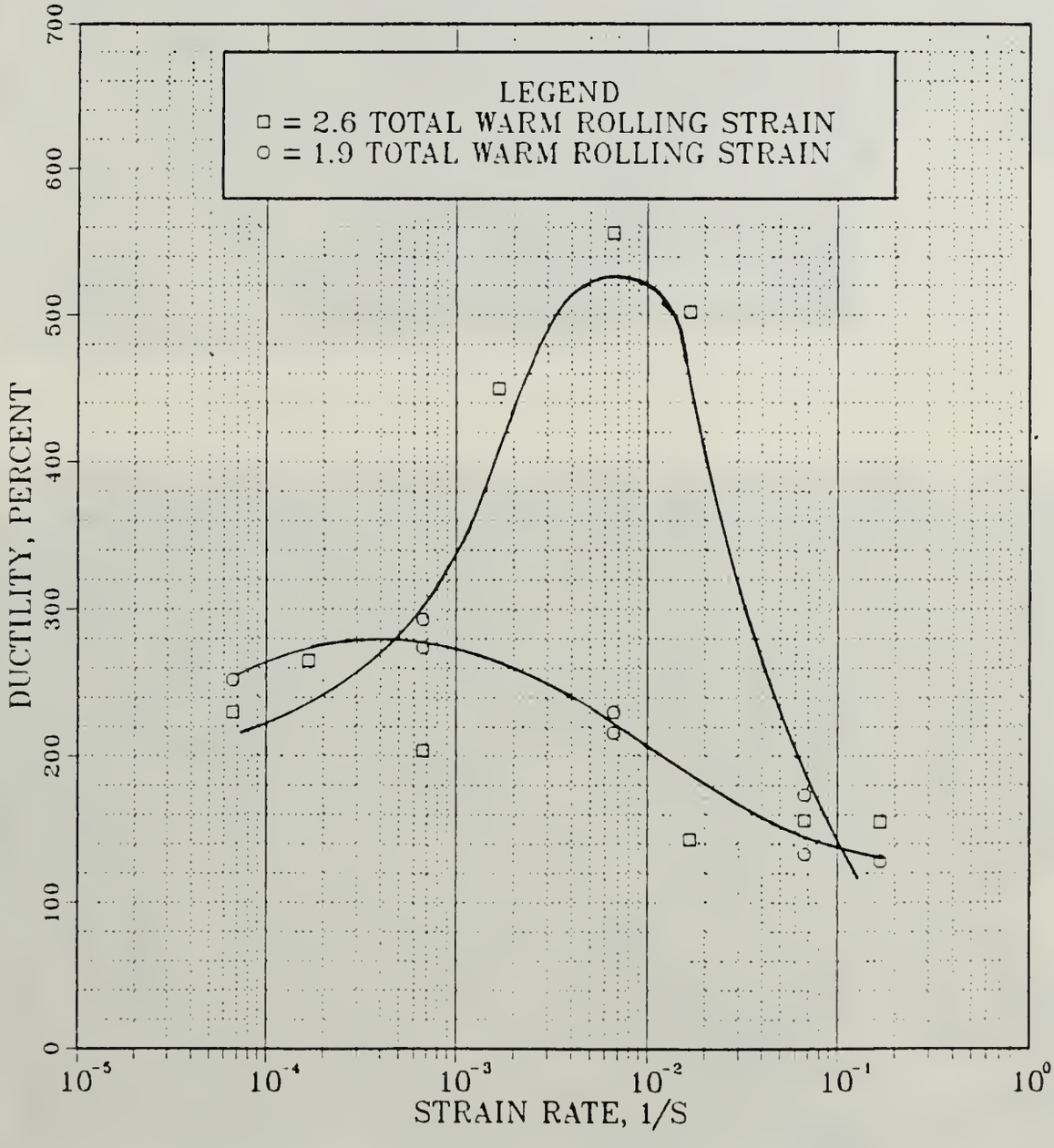

Figure 4.8. Ductility Versus Strain Rate Comparison. The increased total warm rolling strain produces a large increase in peak ductility and an increase in strain rate for peak ductility. Also, peak ductility corresponds to the maximum m-value from the previous data.

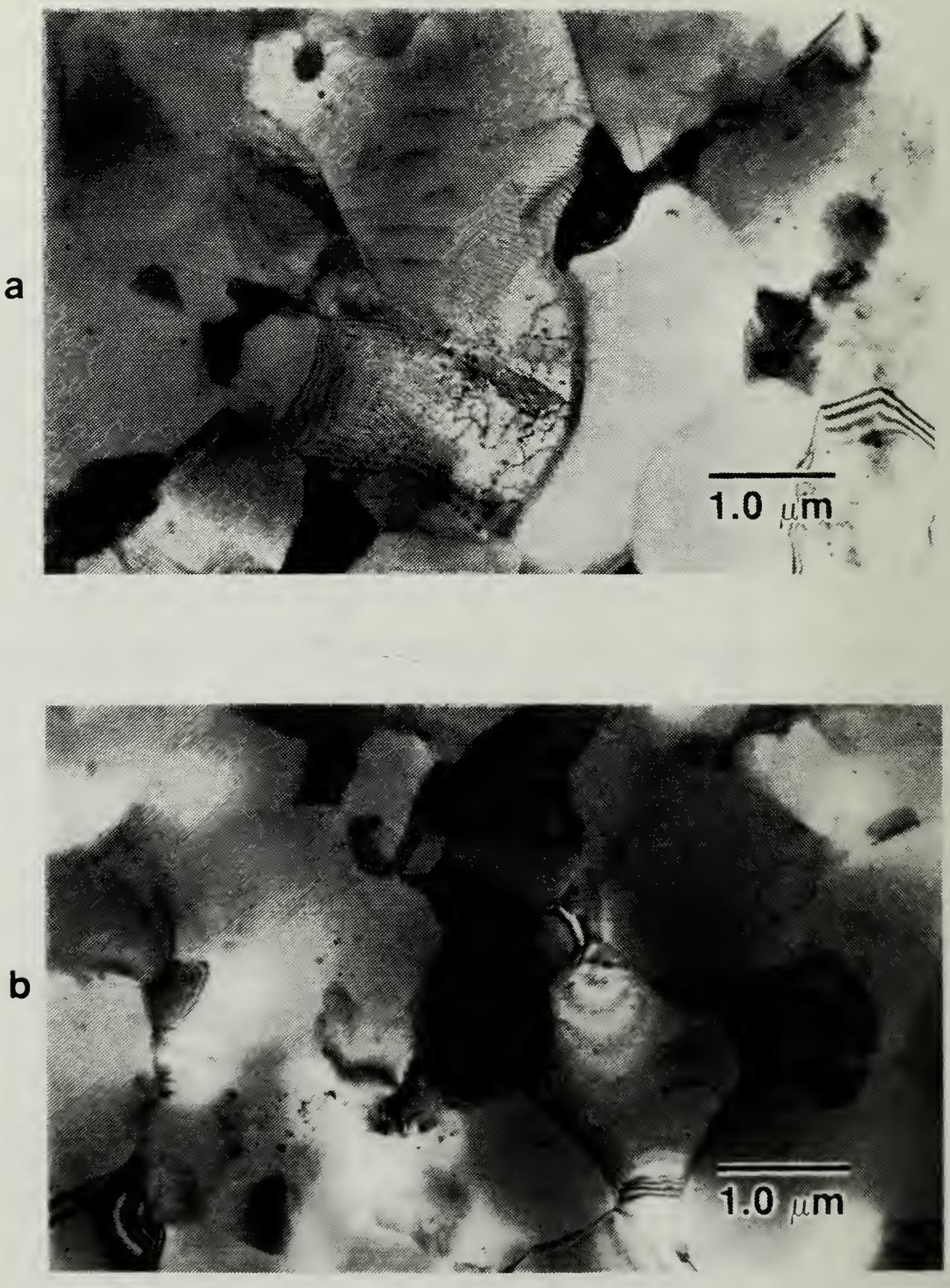

Figure 4.9. A TEM Micrograph Comparison of SPD Tensile Specimen Gage Sections Having a Total Warm Rolling Strain of 1.9(a) and 2.6(b) at a Strain Rate of $6.67 \times 10^{-3} s^{-1}$. The materials experienced elongations of 230% in (a) and 556% in (b).

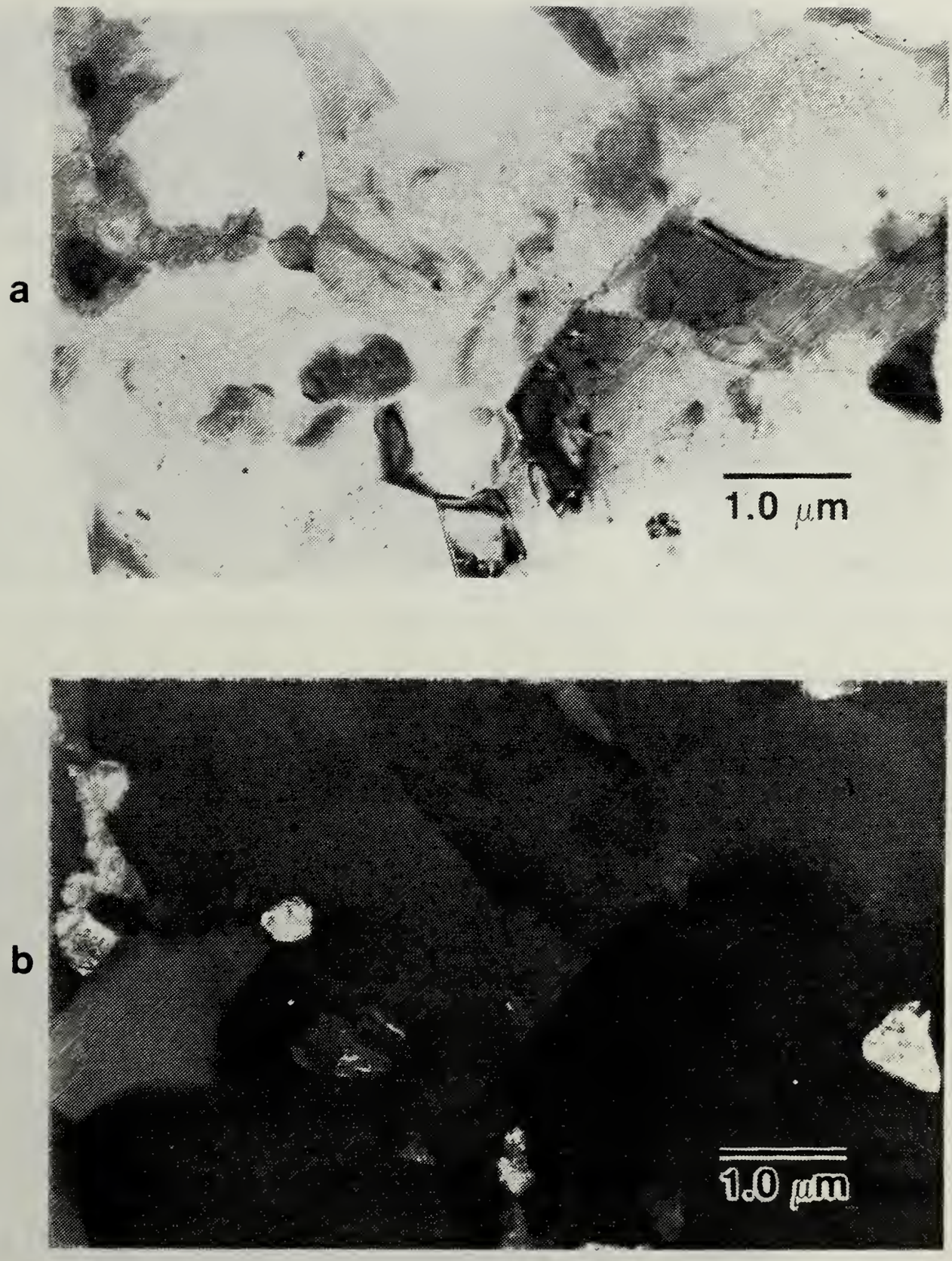

Figure 4.10. A Bright field (a), Dark field (b) Pair of TEM Micrographs Illustrating the Distribution of the β in the Deformed Gage Section of Material Processed to 1.9 Total Warm Rolling Strain and Then Deformed at a Strain Rate of $6.67 \times 10^{-3} s^{-1}$ at 573K (300°C).

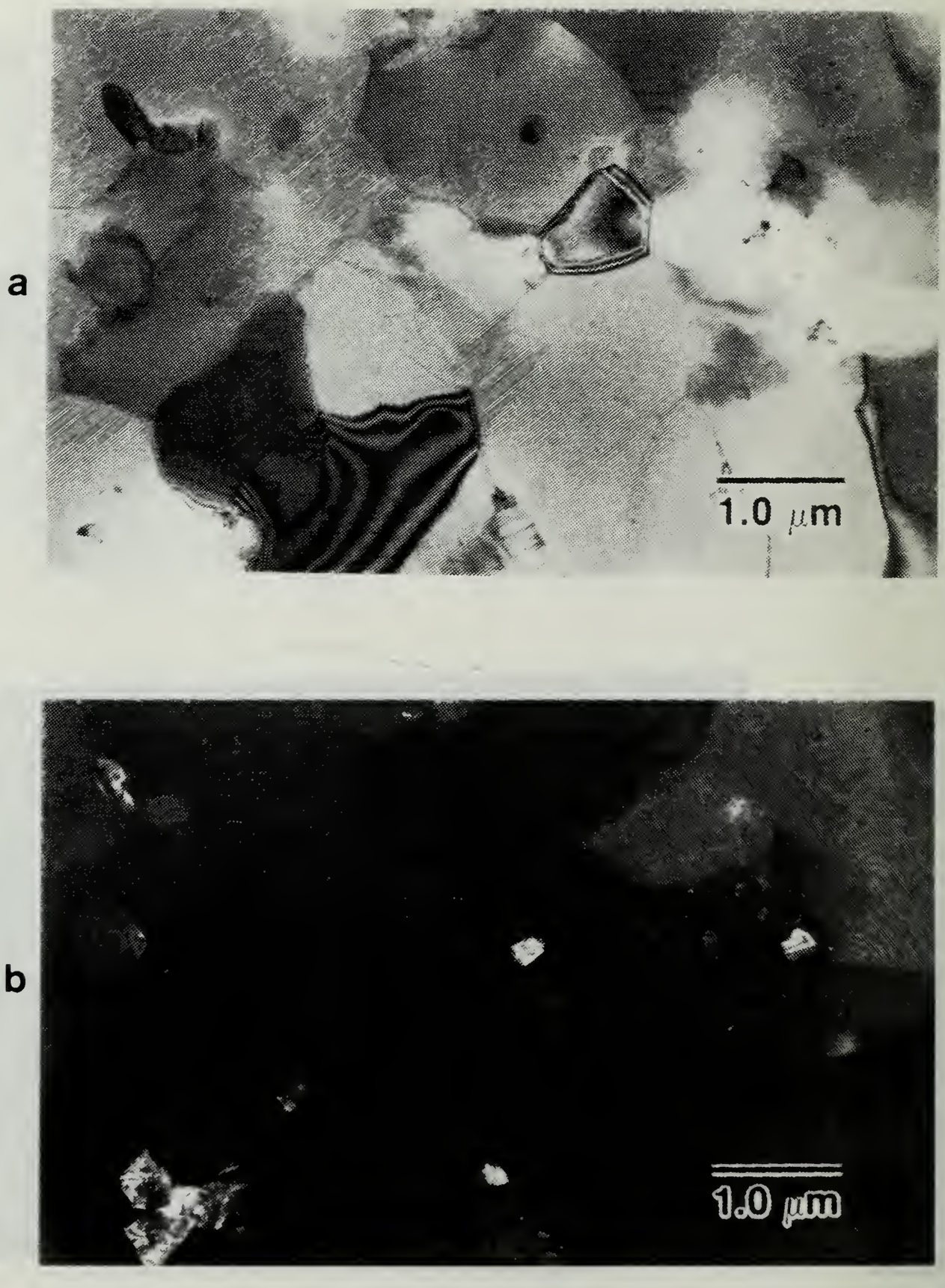

Figure 4.11. A Bright field (a), Dark field (b) Pair of TEM Micrographs Illustrating the Distribution of the β in the Deformed Gage Section of Material Processed to 2.6 Total Warm Rolling Strain and Then Deformed at a Strain Rate of 6.67 x $10^{-3}s^{-1}$ at 573K (300°C).

not great, which would indicate that the microstructures coarsen to an approximately equal point before necking and failure occurs.

Models for superplastic deformation suggest $\dot{\varepsilon}_{spd} \sim \frac{\sigma^2}{d^2}$ where d is the grain size and σ is the stress. The material starting with the finer grain size will be weaker and able to sustain grain coarseing longer before dislocation processes intervene and limit ductility.

The β is credited with the pinning of grain boundaries during SPD thereby slowing down grain growth and coarsening. The greater rolling reduction produced a finer, more uniform β distribution before SPD as mentioned earlier. This supports the theory that β retards grain growth and grain coarsening. Comparisons of Figures 4.10 and 4.11 demonstrate that the β in Oster's material remains larger and less evenly distributed after SPD.

In addition to the microscopy, tensile data demonstrates strain hardening during SPD. True stress versus strain rate data for both 1.9 and 2.6 total warm rolling strains at 0.01, 0.1 and 0.2 true strain are shown in Figures 4.12 and 4.13. Both materials are seen to strain harden with an increase in true strain. This coincides with the grain coarsening seen in the microscopy.

At the onset of deformation the material posses the necessary prerequisites for superplastic behavior. When the specimen is pulled the grains begin to coarsen which results in the strain hardening. According to equation 2.1, as the grain size increases the stress must also increase to maintain a constant strain rate. A point is reached where alternative deformation mechanisms are activated and necking can no longer be as readily resisted and failure follows.

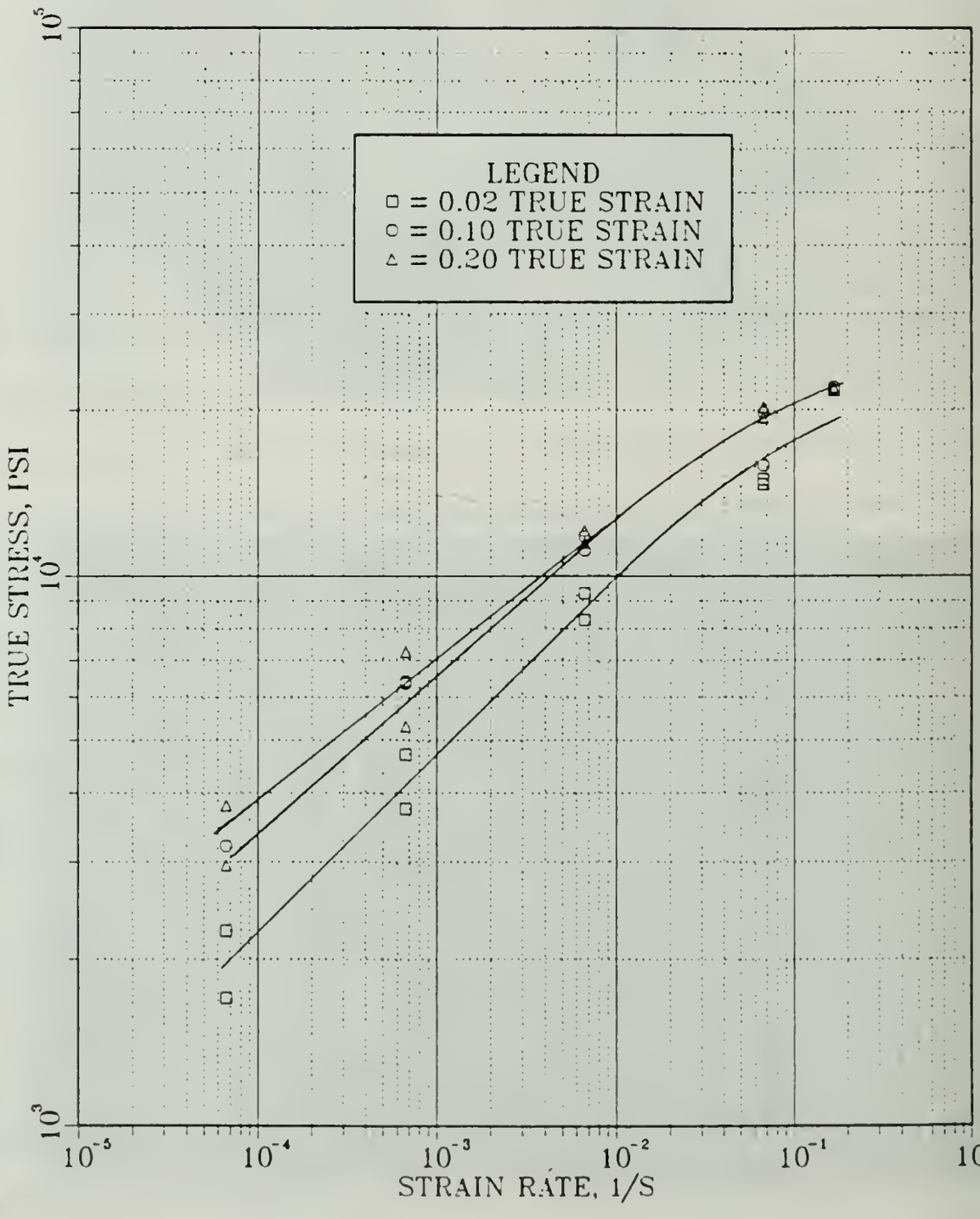

Figure 4.12. True Stress Versus Strain Rate at True Strains of 0.02, 0.1 and 0.2 for the Material With A Total Warm Rolling Strain of 1.9.

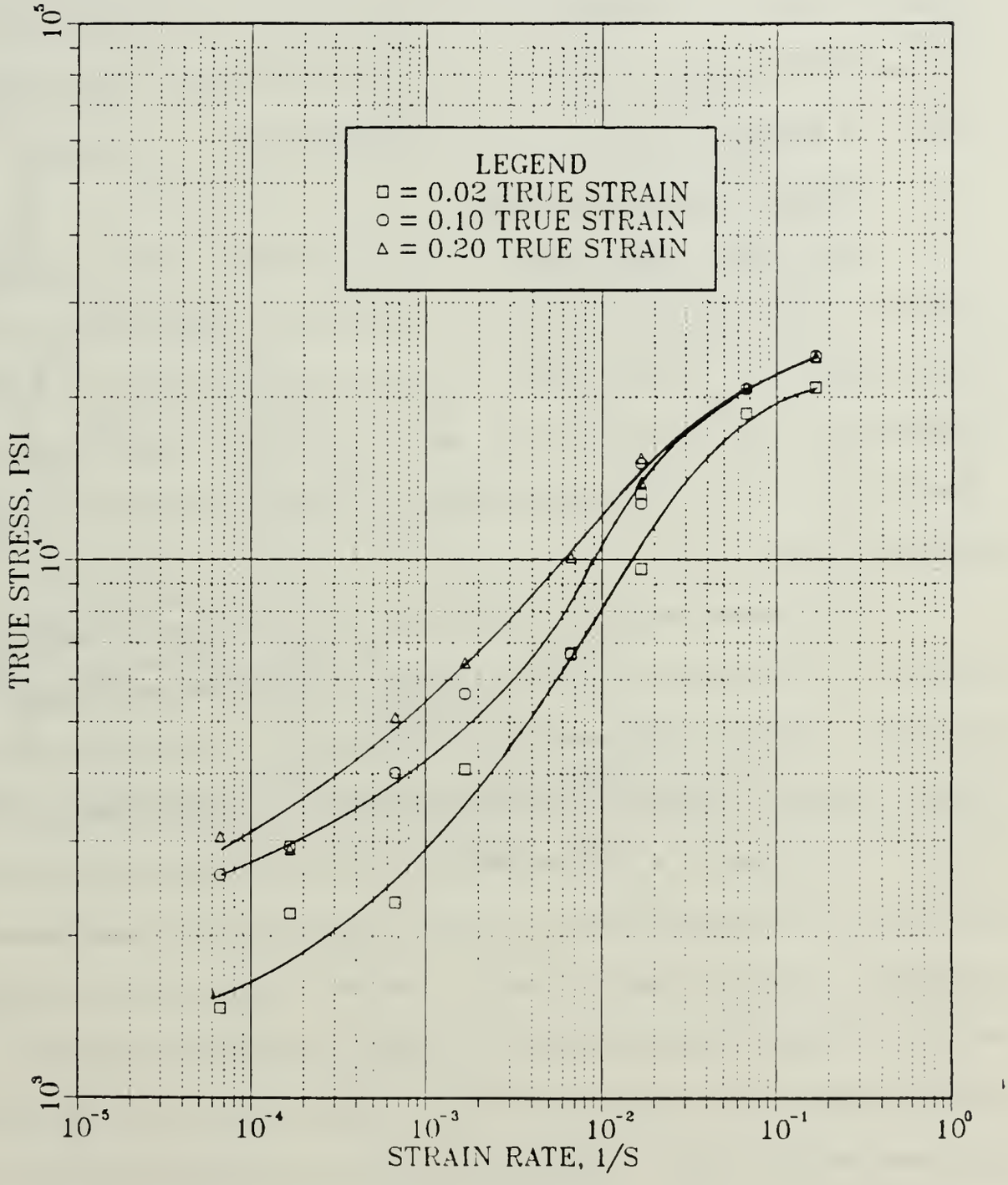

Figure 4.13. True Stress Versus Strain Rate at True Strains of 0.02, 0.1 and 0.2 for the Material With A Total Warm Rolling Strain of 2.6.

B. HEAVIER ROLLING REDUCTION RATE

The effect on superplastic behavior of incresing the reduction per pass, from 1mm to 2.5mm enroute to the 2.6 total warm rolling strain, was investigated as well. Warm working of a second billet, using a heavier 2.5mm per pass, only achieved a 2.25 total strain. An additional rolling pass would have made the material too thin to be usefull for testing and would have produced a total strain in excess of 3.5.

1. Elevated Temperature Tests

True stress versus true strain data for this heavy reduction TMP is provided in Figure 4.14. As before, this data is then used to plot the true stress versus strain rate at 0.1 true strain. Figure 4.15 is a comparison of this information for both the 1mm and 2.5mm per pass reduction schemes. The heavier rolling developed a larger flow stress and a lesser maximum m value ~0.3.

True stress versus strain rate at 0.02, 0.1 and 0.2 true stress, Figure 4.16, show that the 2.5mm per pass process also undergoes strain hardening. The extent of this strain hardening, as indicated by the flow stress, was less than for the material rolled at 1mm per pass. With the larger rolling passes a greater amount of strain hardening would have been anticipated as a reflection of a finer initial structure and greater grain coarsening. The fact that it didn't increase as much as it was expected is not fully understood at this time. Ductility as shown in Figure 4.17 is not as high as the 1mm per pass TMP produced and it is also not as consistant at the lower strain rates. The lesser ductility is constant with the lower m-value.

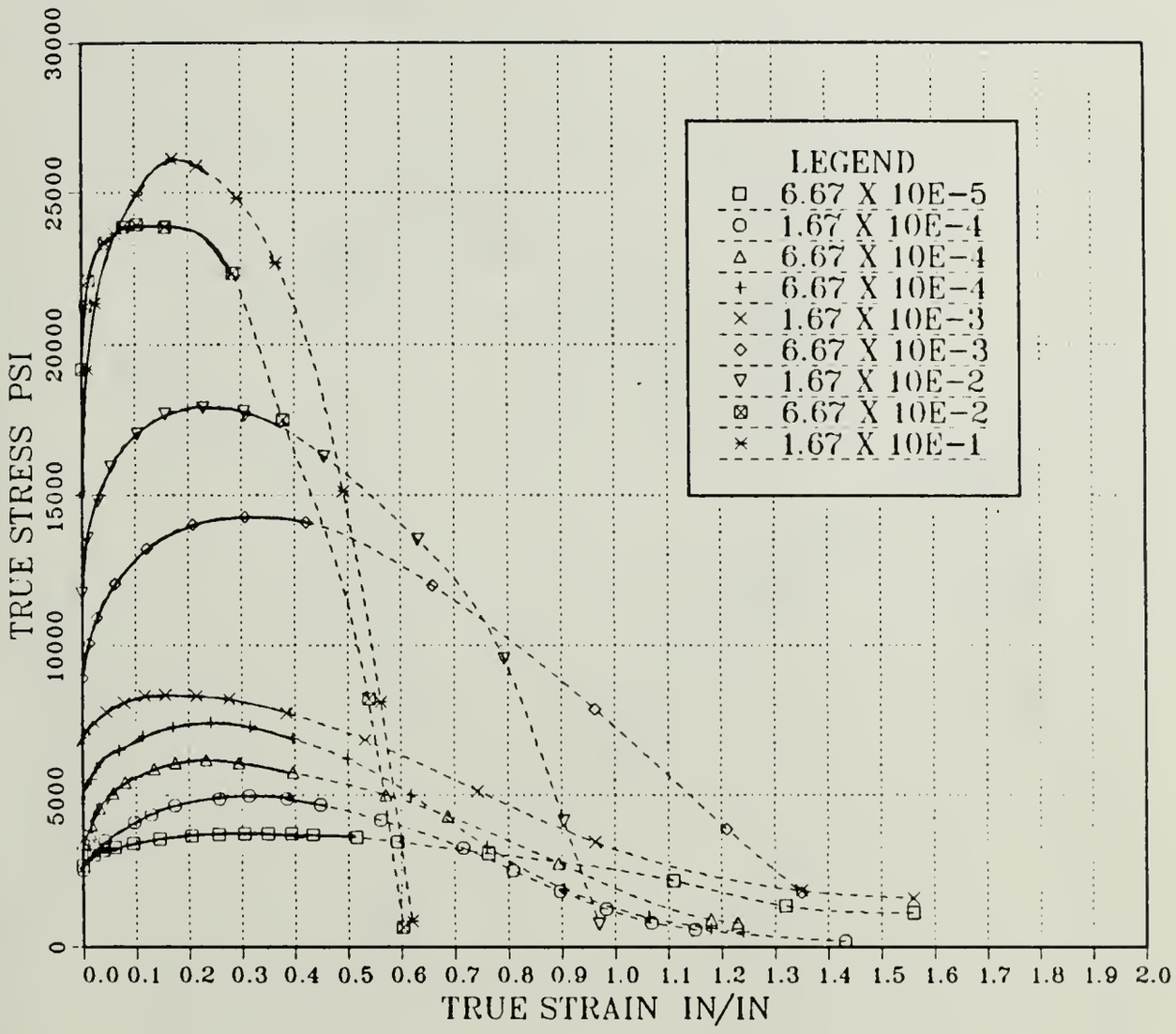

Figure 4.14. True Stress Versus True Strain for Deformation at 573K (300°C). The 2.5mm reduction per pass during rolling produced a total strain of 2.25. Strain rates varied from $10^{-5}S^{-1}$ to $10^{-1}S^{-1}$ as indicated.

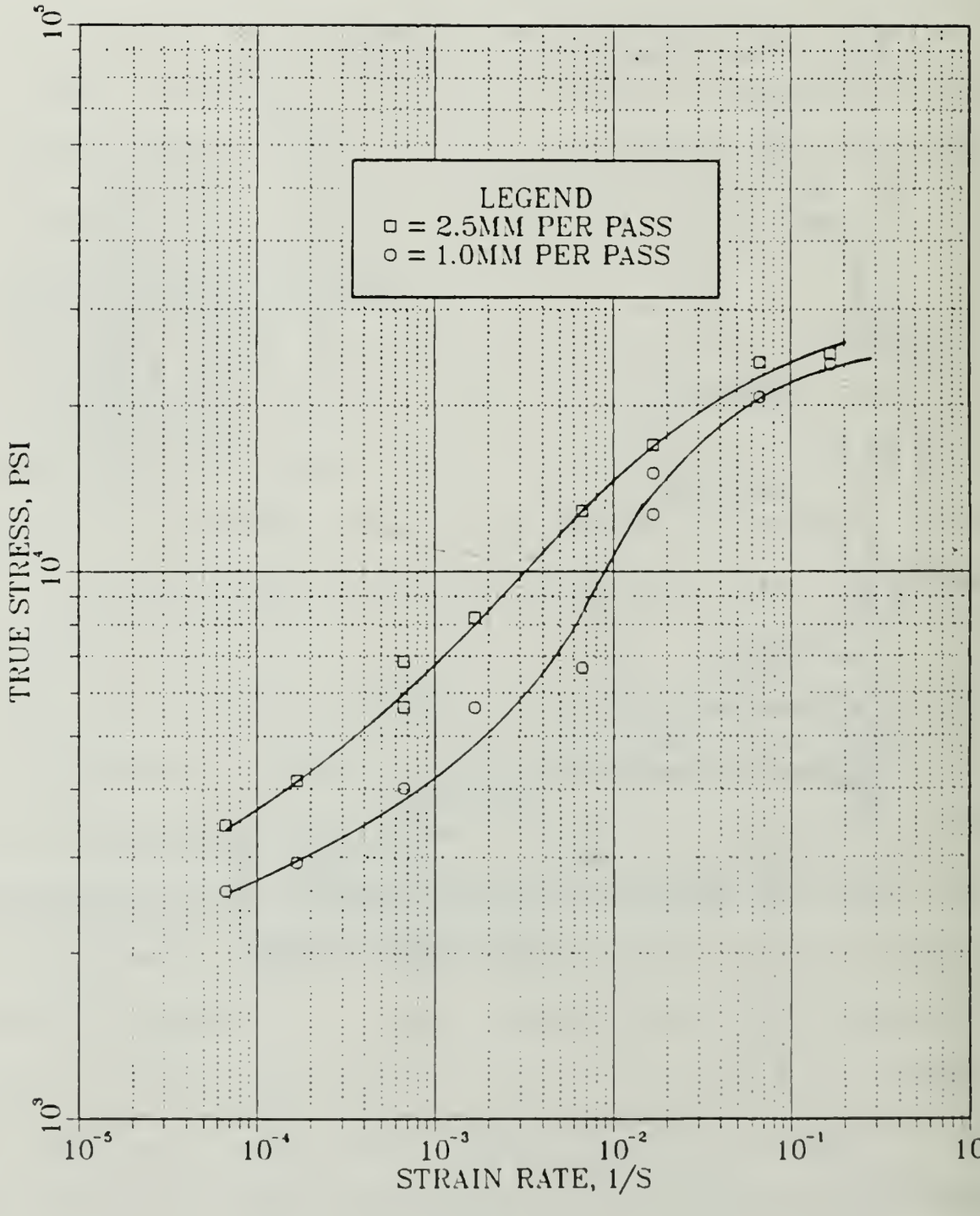

Figure 4.15. True Stress Versus Strain Rate for the Light and Heavy Rolling at 0.1 True Strain. The 2.5mm reduction per pass reached a total warm rolling strain of 2.25 compared to 2.6 for the 1mm reduction per pass. Heaviewr rolling developed a larger flow stress but comparison is difficult as both the total warm rolling strains and reduction rates differ.

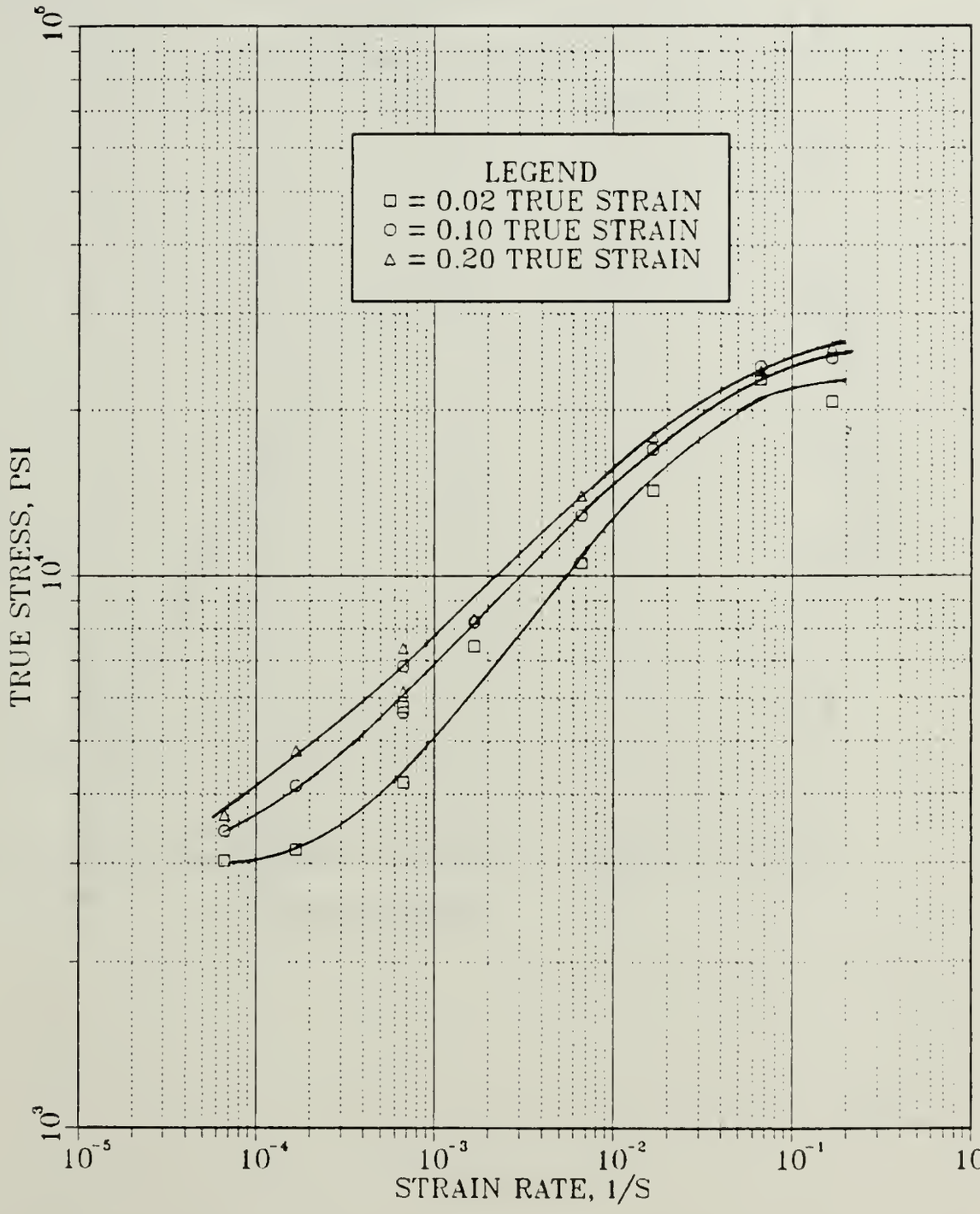

Figure 4.16. True Stress Versus Strain Rate at True Strains of 0.02, 0.1 and 0.2 for the 2.5mm Rolling Reduction Process.

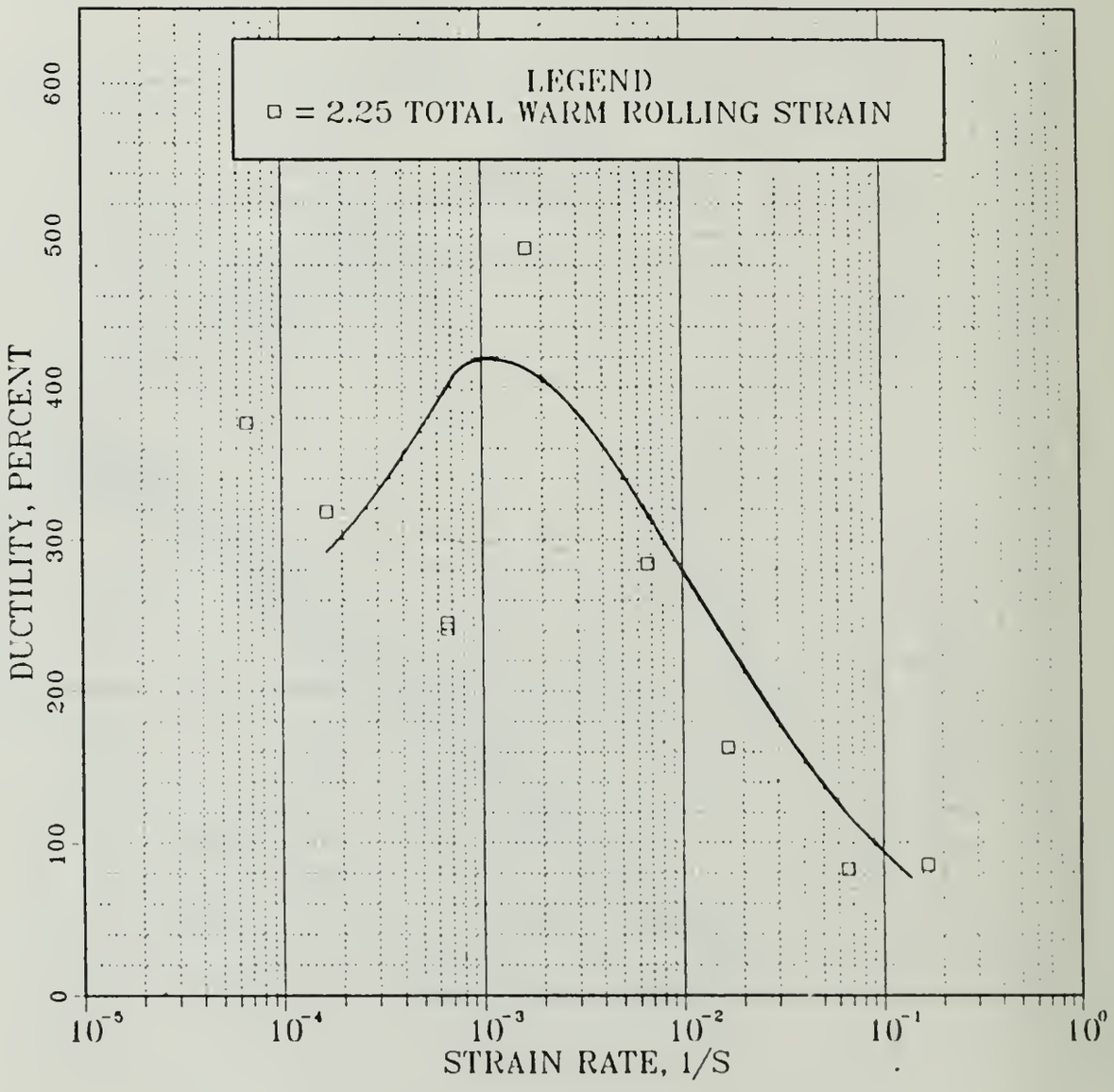

Figure 4.17. Ductility Versus Strain Rate for 2.5mm Rolling Reduction. A total warm rolling strain of 2.6 was desired but not achieved; comparison with material rolled with 1mm per pass is difficult as both the total warm rolling and reduction per pass differ.

Direct comparison of flow stress, m value and ductility of the 1mm and 2.5mm per pass processes is difficult because the total warm rolling strain and reduction per pass differed. Attributing a response to a specific variable was not possible when two of the variables were changed in the TMP.

V. CONCLUSIONS

1. Increasing the total warm rolling strain from 1.9 to 2.6 for the Al-8.0%Mg-0.5%Li-0.23%Zr alloy resulted in a more fully superplastic response.

2. The maximum value of the strain rate sensitivity coefficient increased from 0.31 in the material experiencing the 1.9 total warm rolling strain to 0.5 in the 2.6 total warm rolling strain sample.

3. The increase in total warm rolling strain from 1.9 to 2.6 resulted in the peak ductilities occuring at higher strain rates, from $10^{-4}S^{-1}$ to $10^{-1}S^{-1}$.

4. Transmission electron microscopy reveals that the increase in total warm rolling strain produced a finer, more equiaxed grain structure with a less coarse, more evenly distributed second phase (β, Al_8Mg_5). This fact is evident for both before and after SPD.

5. A greater warm rolling strain on the alloy produces a decrease in flow stress during superplastic tests.

6. Transmission electron microscopy supports the continuous recrystallization model where a high initial dislocation density recovers and coalesces into a fine grain, relatively dislocation free and stable microstructure.

7. Use of 2.5mm reduction per pass gives a higher resultant flow stress in subsequent testing when compared to 1mm reduction per pass during warm

rolling. This also resulted in a decrease in the strain rate sensitivity coefficient from 0.5 to 0.3.

VI. SUGGESTIONS FOR FUTURE RESEARCH

The result of this thesis show that a Lithium-containing alloy can behave superplastically. The increase in the total warm rolling strain during TMP improves the subsequent microstructure so as to improves the superplastic response of the material. It is therefore suggested that the following research areas be addressed:

1. Study the effect of the greater total warm rolling strain on the alloys with higher Mg and Li contents than the alloy in this study, namely up to 10% Mg and 1% Li.

2. A detailed microstructural investigation, including misorientation studies, to confirm the mode of recrystallizatrion in the Al-Mg-Li-Zr alloys.

3. Investigate the effect of the more severe working scheme (i.e. a rolling strain rate at 2.5mm per pass) to a 2.6 total warm rolling strain.

4. Following the observation that Al_3Li precipitates upon cooling, study the potential for precipitation hardening to enhance the ambient temperature properties of the Lithium-containing alloys.

LIST OF REFERENCES

1. Underwood, E. E., "A Review of Superplasticity and Related Phenomena," Journal of Metals, pp. 914-919, 1962.

2. Lipsus, H., Stock, J. and Shames, A., "Secondary Fabrication Techniques for Superplastically Formed Aluminum," Superplasticity in Aerospace-Aluminum, Conference Proceedings, p. 403, July 1985.

3. Oster, S. B., Effect of Thermomechanical Processing on the Elevated Temperature Behavior of Lithium-Containing High-Mg, Al-Mg Alloys, M.S. Thesis, Naval Postgraduate School, Monterey, California, June 1985.

4. Lee, E. W., McNelley, T. R. and Stengel, A. F., "The Influence of Thermomechanical Processing Variables on Superplasticity in a High-Mg, Al-Mg Alloy," Metallurgical Transactions A, Vol. 17A, pp. 1043-1050, 1986.

5. Mondolfo, L. F., Aluminum Alloys: Structure and Properties, pp. 312-313, Butterworth, 1976.

6. Massalski, T. B., Binary Alloy Phase Diagrams, Vol. 1, pp. 129-130, American Society for Metals, 1986.

7. Wadsworth, J., Pelton, A. R. and Lewis, R. E., "Superplastic Al-Cu-Li-Mg-Zr Alloys," Met. Trans., Vol. 16A, pp. 2319-2332, December 1985.

8. Brosilow, R., "Aircraft Bodies: New Joining Processes," Welding Design and Fabrication, Vol. 58, p. 57, March 1985.

9. Sigili, C. and Sanchez, J. M., "Calculation of Phase Equilibrium in Al-Li Alloys," Acta Metallurgica, Vol. 34, pp. 1021-1028, 1986.

10. Sherby, O. D. and Wadsworth, J., "Development and Characterization of Fine-Grained Superplastic Materials," in Deformation Processing and Structure, G. Krauss, Ed., American Society for Metals, pp. 355-390, 1984.

11. Andrews, J. N., A Calorimetric Study of the Microstructures of a Thermomechanically Processed Al-10.0% Mg-0.1%Zr Alloy, M. S. Thesis, Naval Postgraduate School, Monterey, California, September 1986.

12. Hales, S. J. and McNelley, T. R., "Microstructural Evaluation by Continuous Recrystallization in a Superplastic Al-Mg Alloy," submitted to Acta Metallurgica, March 1986.

13. McNelley, T. R. and Garg, A., "Development of Structure and Mechanical Properties in Al-10.2%Mg by Thermomechanical Processing," Scripta Met., Vol. 18, pp. 917-920, 1984.

14. Self, R. J., The Effect of Alloy Additions on Superplasticity in Thermomechanically Processed High Magnesium Aluminum Magnesium Alloys, M. S. Thesis, Naval Postgraduate School, Monterey, California, 1984.

15. Berthold, D. B., Effect of Temperature and Strain Rate on the Microstructure of a Deformed, Superplastic Al-10%Mg-0.1%Zr Alloy, M. S. Thesis, Naval Postgraduate School, Monterey, California, June 1985.

16. Alcamo, M. E., Effect of Strain and Strain Rate on the Microstructure of a Superplastically Deformed Al-10%Mg-0.1%Zr Alloy, M. S. Thesis, Naval Postgraduate School, Monterey, California, June 1985.

17. Anamet Laboratories Inc., Berkeley, California, private communication, February 1986.

18. Metals Handbook, 8th Ed., Vol. 8, p. 261, American Society for Metals, 1973.

19. Lee, E. W. and McNelley, T. R., "Microstructure Evolution During Processing and Superplastic Flow in a High-Mg, Al-Mg Alloy," Mater. Sci. Eng. J., in press.

20. Wert, J. A., "Thermomechanical Processing of Heat Treatable Aluminum Alloys for Grain Size Control," Microstructural Control in Aluminum Alloys, pp. 67-94, The Metallurgical Society, Inc., 1986.

APPENDIX

MECHANICAL TEST DATA

1mm Per Pass

TEMP (C)	TOTAL STRAIN	STRAIN RATE (sec^{-1})	TRUE STRESS AT 0.1 TRUE STRAIN Ksi	DUCTILITY (Percent Elong.)
300	-1.9	1.67×10^{-1}	22.00	128
		6.67×10^{-2}	19.81	133
			15.90	174
		6.67×10^{-3}	11.15	230
			11.79	216
		6.67×10^{-4}	6.35	274
			6.40	293
		6.67×10^{-5}	3.21	252
	-2.6	1.67×10^{-1}	23.80	155
		6.67×10^{-2}	20.70	156
		1.67×10^{-2}	15.10	143
			12.70	502
		6.67×10^{-3}	6.67	556
		1.67×10^{-3}	5.64	450
		6.67×10^{-4}	4.02	204
		1.67×10^{-4}	2.93	265
		6.67×10^{-5}	2.60	230

2.5mm Per Pass

300	-2.25	1.67×10^{-1}	24.84	86
		6.67×10^{-2}	23.97	83
		1.67×10^{-2}	17.00	162
		6.67×10^{-3}	12.87	284
		1.67×10^{-3}	82.30	491
		6.67×10^{-4}	6.84	245
			5.64	241
		1.67×10^{-4}	4.14	319
		6.67×10^{-5}	3.44	377

INITIAL DISTRIBUTION LIST

		No. Copies
1.	Defense Technical Information Center Cameron Station Alexandira, Virginia 22304-6145	2
2.	Library, Code 0142 Naval Postgraduate School Monterey, California 93943-5002	2
3.	Department Chairman, Code 69Hy Department of Mechnical Engineering Naval Postgraduate School Monterey, California 93943-5000	1
4.	Professor T. R. McNelley, Code 69Mc Department of Mechnical Engineering Naval Postgraduate School Monterey, California 93943-5000	5
5.	Dr. S. J. Hales, Code 69Ha Department of Mechnical Engineering Naval Postgraduate School Monterey, California 93943-5000	1
6.	LT Benjamin W. Sanchez 7 Bellrose Avenue Cortland, New York 13045	5
7.	LCDR Stephen B. Oster 110 Teri Court, N.E. Bremerton, Washington 98310	1
8.	Dr. J. Waldman, Code 606 Naval Air Development Center Warminster, Pennsylvania 18974	1
9.	Dr. Eui-Whee Lee, Code 6063 Naval Air Development Center Warminster, Pennsylvania 98310	1
10.	Dr. Lewis E. Sloter, Code AIR 931A Naval Air Systems Command Headquarters Washington, District of Columbia 20361	1

Thesis
S15783
c.1

Sanchez
Processing and super-
plasticity in lithium-
containing Al-Mg alloys.